NASA/TM—2016–219156

Category B Plastic Pane Testing for JSC 66320 Rev A Requirements Verifiable Through Acceptance Testing

Robert C. Youngquist
NASA Kennedy Space Center, Florida

Mark Nurge
NASA Kennedy Space Center, Florida

Susan Danley
NASA Kennedy Space Center, Florida

Miles Skow
NASA Johnson Space Center, Texas

August 2016

NASA/TM—2016–219156

NASA STI Program…in Profile

Since its founding, NASA has been dedicated to the advancement of aeronautics and space science. The NASA Scientific and Technical Information (STI) program plays a key part in helping NASA maintain this important role.

The NASA STI Program operates under the auspices of the Agency Chief Information Officer. It collects, organizes, provides for archiving, and disseminates NASA's STI. The NASA STI program provides access to the NASA Aeronautics and Space Database and its public interface, the NASA Technical Reports Server, thus providing one of the largest collections of aeronautical and space science STI in the world. Results are published in both non-NASA channels and by NASA in the NASA STI Report Series, which includes the following report types:

- TECHNICAL PUBLICATION. Reports of completed research or a major significant phase of research that present the results of NASA programs and include extensive data or theoretical analysis. Includes compilations of significant scientific and technical data and information deemed to be of continuing reference value. NASA counterpart of peer-reviewed formal professional papers but has less stringent limitations on manuscript length and extent of graphic presentations.

- TECHNICAL MEMORANDUM. Scientific and technical findings that are preliminary or of specialized interest, e.g., quick release reports, working papers, and bibliographies that contain minimal annotation. Does not contain extensive analysis.

- CONTRACTOR REPORT. Scientific and technical findings by NASA-sponsored contractors and grantees.

- CONFERENCE PUBLICATION. Collected papers from scientific and technical conferences, symposia, seminars, or other meetings sponsored or cosponsored by NASA.

- SPECIAL PUBLICATIONS. Scientific, technical, or historical information from NASA programs, projects, and missions, often concerned with subjects having substantial public interest.

- TECHNICAL TRANSLATION. English-language translations of foreign scientific and technical material pertinent to NASA's mission.

Specialized services also include creating custom thesauri, building customized databases, organizing and publishing research results.

For more information about the NASA STI program, see the following:

- Access the NASA STI program home page at http://www.sti.nasa.gov

- E-mail your question via the Internet to help@sti.nasa.gov

- Fax your question to the NASA STI Help Desk at 443-757-5803

- Telephone the NASA STI Help Desk at 443-757-5802

- Write to:
  NASA Center for Aerospace Information (CASI)
  7115 Standard Drive
  Hanover, MD 21076-1320

NASA/TM—2016–219156

Category B Plastic Pane Testing for JSC 66320 Rev A Requirements Verifiable Through Acceptance Testing

Robert C. Youngquist
NASA Kennedy Space Center, Florida

Mark Nurge
NASA Kennedy Space Center, Florida

Susan Danley
NASA Kennedy Space Center, Florida

Miles Skow
NASA Johnson Space Center, Texas

National Aeronautics and
Space Administration

Kennedy Space Center

August 2016

Acknowledgments

We would like to acknowledge helpful discussions with Lynda Estes and Hannah Bradley of the Johnson Space Center and Ken Tedjojuwono and William Humphries of the Langley Research Center. These discussions helped us in understanding the requirements and in generating appropriate measurement processes to achieve the results intended. We would also like to acknowledge help from Benjamin Wallace on the birefringence measurement error analysis.

Available from:

NASA Center for Aerospace Information
7115 Standard Drive
Hanover, MD 21076-1320

National Technical Information Service
5301 Shawnee Road
Alexandria, VA 22312

Available in electronic form at http://www.sti.nasa.gov.

Contents

Figures

Tables

Abbreviations, Acronyms, and Symbols

µm	micrometer (micron)
µV	microvolt
arcmin	minute of arc
ASTM	ASTM International
CaF2	calcium fluoride
CIE	International Commission on Illumination
cm	centimeter
CW	clockwise
DC	direct current
Hz	hertz
in	inch
JFET	junction gate field-effect transistor
JSC	Johnson Space Center
LED	light-emitting diode
m	meter
mm	millimeter
mV	millivolt
mW	milliwatt
NASA	National Aeronautics and Space Administration
nm	nanometer
op amp	operational amplifier
rad	radian
rms	root mean square
TM	Technical Memorandum
W	watt

1 OVERVIEW

JSC 66320, Revision A, O*ptical Property Requirements for Glasses, Ceramics, and Plastics in Spacecraft Window Systems*, lists several quantitative requirements that spacecraft windowpanes must meet. Recently, we were asked to establish a capability at the Kennedy Space Center to perform these measurements on category B plastic panes, i.e., plastic panes that could be used on a spacecraft for long-focal-length photography and piloting. Two of the criteria, normal wavefront and 30-degree wavefront attributes, can be measured with existing equipment and processes (see NASA TM NESC-RP-14-00951, April 2016) and are not discussed in this document. However, the other six criteria—haze, wedge angle, birefringence, reflectance, transmittance, and color balance—required substantial development and are the subject of this document.

In this document, we do not discuss the rationale behind the requirements, but we did engage in discussions with the authors of JSC 66320 in order to better understand the requirements and the verifications being imposed on windows and their testing. Accordingly, this document presents our best understanding of the requested requirements and verifications. We also present our methodology for performing each of the six measurements, along with applicable mathematics and a description, with photos, of the hardware used. In addition, we supply the results of a test on a low-quality in-house plastic window as an example of the system operation.

Only requirements that can be met by acceptance test and analysis, as opposed to optical inspection, are considered in this document.

2 GENERAL COMMENTS

The following concerns or assumptions apply to all of the measurements.

a. As part of our prior work on developing a wavefront measurement capability, we constructed an X-Y scanning system to hold individual windowpanes or complete two- or three-pane window stacks and then position them horizontally and vertically to high accuracy. This scanning system, shown in Figure 1, is mounted on a 4 foot × 10 foot research-grade optical table with an active vibration isolation system.

   Since the windowpanes require wavefront measurements, they must be mounted to the X-Y scanner so that the Zygo interferometer, also shown in Figure 1, can be used to make measurements. In order to minimize handling and to take advantage of the scanner, we decided that six measurements would be made on the window while it is mounted to this scanner. Consequently, all of the hardware associated with the six measurements must be installed on this optical table and configured to be compatible with the existing system and the clearance spaces around the windowpane.

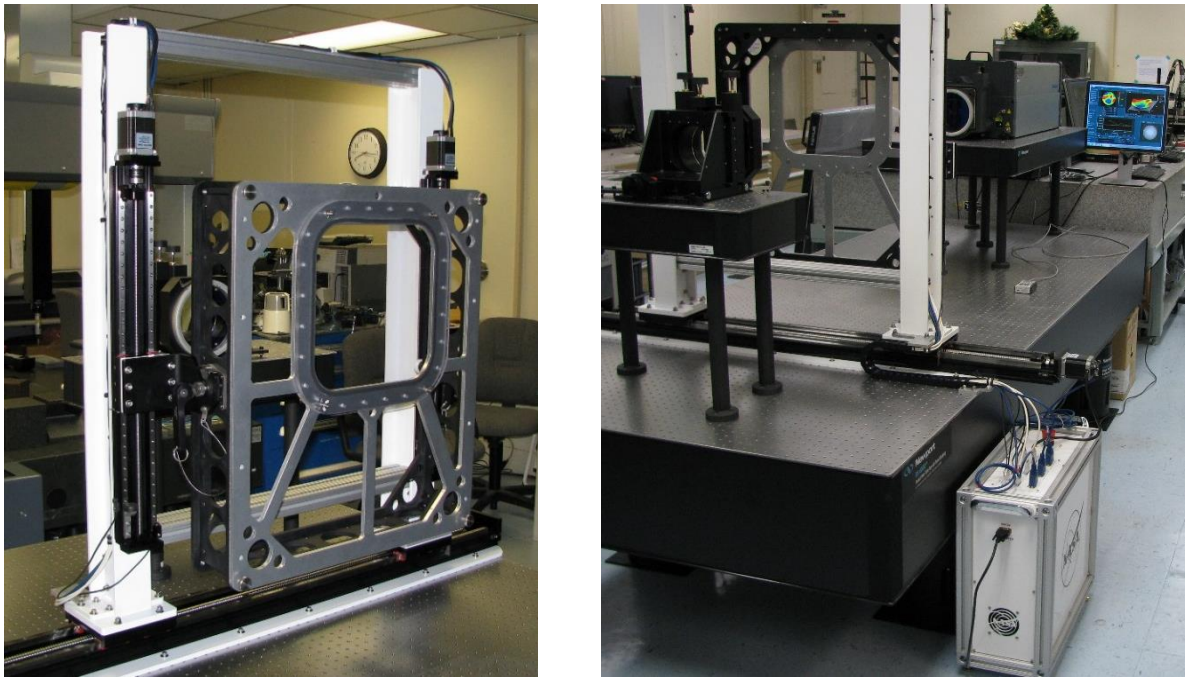

Figure 1. Left, X-Y scanner that the pane will be attached to; right, 4- × 10-foot optical table with the scanner and the Zygo interferometer

b. We assume that the windowpane under test cannot be touched during testing. For most of the measurements this is not a concern, but a couple of the requested ASTM standards quoted in the verification section of JSC 66320 require contact with the pane. We requested that these verification procedures be modified so that the windowpanes would not come in contact with the mounted pane.

c. We assume that substantial clearance in front of the scanner is needed to ensure that it does not make contact with any of the measurement equipment while the windowpane is being loaded onto the scanner.

d. In all of the tests, we will minimize the exposure of the pane to excessive infrared or ultraviolet radiation. Some of the ASTM standards use intense halogen bulbs, and their emission could be harmful if it were focused on the plastic windowpane due to absorption in those bands.

e. Very few of the requirements listed in JSC 66320, Revision A, provide an error range, so we will assume that wherever it is reasonable, the measurement accuracy should be such that the least significant digit provided by the requirement is achieved 95% of the time. For example, if a requirement calls for 82% transmission, then we assume that means 82±0.5% to two standard deviations. For some measurements, this cannot be achieved; we will discuss those situations in detail.

f. For haze, transmission, and birefringence measurements, it is necessary to use a photodetector and current-to-voltage conversion circuitry. For all of our measurements, we used large-area photodetectors, such as the Thor Labs SM1PD1A mounted silicon photodiode, followed by circuitry similar to that shown in Figure 2. The specific values of the components vary with the specific measurement, depending on the amount of light available.

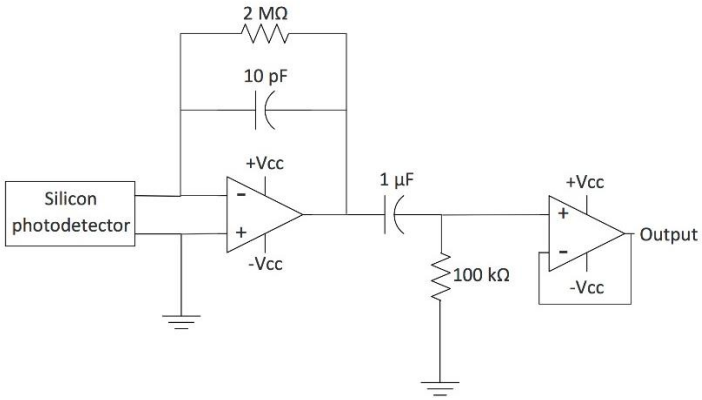

Figure 2. Current-to-voltage converter and high-pass filter and buffer circuit.

This circuitry takes the current generated by the photodetector and forces it through the feedback resistor of a JFET op amp (we used a TL082). The output from this first op amp has a DC offset on it, which is removed by a high-pass filter. After that, the signal is buffered and sent to a National Instruments data acquisition system.

For all of our measurements, the light sources are modulated, either directly in the case of LEDs and lasers or through the use of a chopper for the halogen lightbulb used in the transmission measurements. Our modulation frequency is typically 200 Hz. (For the birefringence measurement, two LEDs are running simultaneously so that one is running at 200 Hz and one at 250 Hz). This frequency range was chosen because it reduces $1/f$ noise substantially, cuts out much of the room light signal (but not all), yet is low enough that a chopper wheel can reach it and substantial amplification is achieved within the gain-bandwidth product of the op amp.

Normally a lock-in amplifier would be used to extract the 200 Hz signal from the electrical signal; instead we have decided to use a LabVIEW digital signal processing algorithm. We acquire 8000 samples per second from the electrical signal and digitally extract the 200 Hz (or 250 Hz) signal. We have shown this approach does not have the resolution of a dedicated lock-in amplifier, but for the measurements given in this document, it provides sufficient performance. The main advantage of this approach is that only one system, composed of a data acquisition module and computer, is needed to access multiple voltages, process them, and save the results.

3 HAZE

Sections 3.5.4.1 and 4.5.4.1 of JSC 66320, Revision A, provide the requirement that "For all glass and category B plastic windowpanes, the transmission haze after all coatings have been applied shall be less than 0.5 percent" and the verification statement, "This requirement shall be verified by acceptance test per ASTM D1003, *Standard Test Method for Haze and Luminous Transmittance of Transparent Plastics*, and/or analysis."

3.1 Discussion

ASTM D1003 states that "the specimen is placed against the entrance port of the integrating sphere," and since this requires contact with the pane, the measurement process must be modified. The sketch shown in Figure 3, taken from ASTM D1003, shows the standard approach with the specimen placed against the integrating sphere so that most of the scattered light is captured.

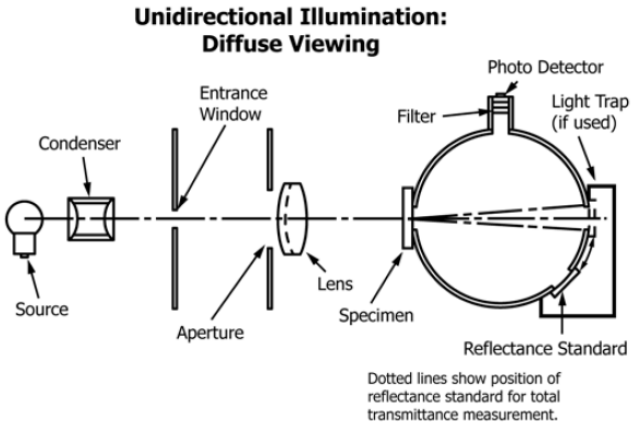

Figure 3. ASTM hazemeter system sketch

We propose to use a modified version of the approach described in ASTM D1003, which will prevent optical components from coming into contact with the pane being examined. Figure 4 shows this approach. Just as in ASTM D1003, a light source is collimated and launched through the specimen under test. We chose to use a laser with an aperture in order to ensure that the beam is within the clear area of the haze standard and that stray light from the laser is blocked from the measurement. What is different from ASTM D1003 is that we are proposing to measure the scattered light in only two scattering directions and not in all directions. We will place a 1% haze reference standard in the pane location and then compare the reading from the pane with that measured from the reference standard and estimate the haze measurement from those readings.

The calibrated haze standard, shown in Figure 5, was purchased from Hunter Labs and is calibrated to be 0.85±0.26 (2σ). This means that there is a 95% confidence that the haze from this standard is between 0.59 and 1.11, but this raises a concern. The requirement is that the pane have less than 0.5% haze, which means that this measurement should be to an accuracy of ±0.1 (2σ), but the calibrated standard is only accurate to ±0.26 (2σ). Consequently, our assumption as to measurement accuracy cannot be achieved for this case. We can only make the measurement and indicate a probability of meeting the requirement.

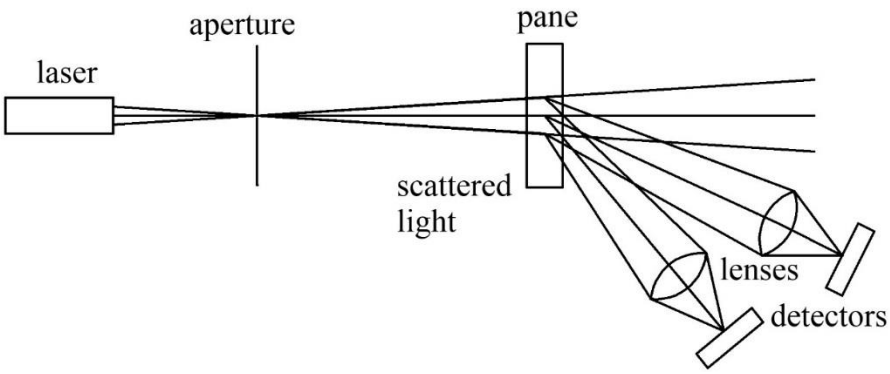

Figure 4. Noncontact haze measurement approach

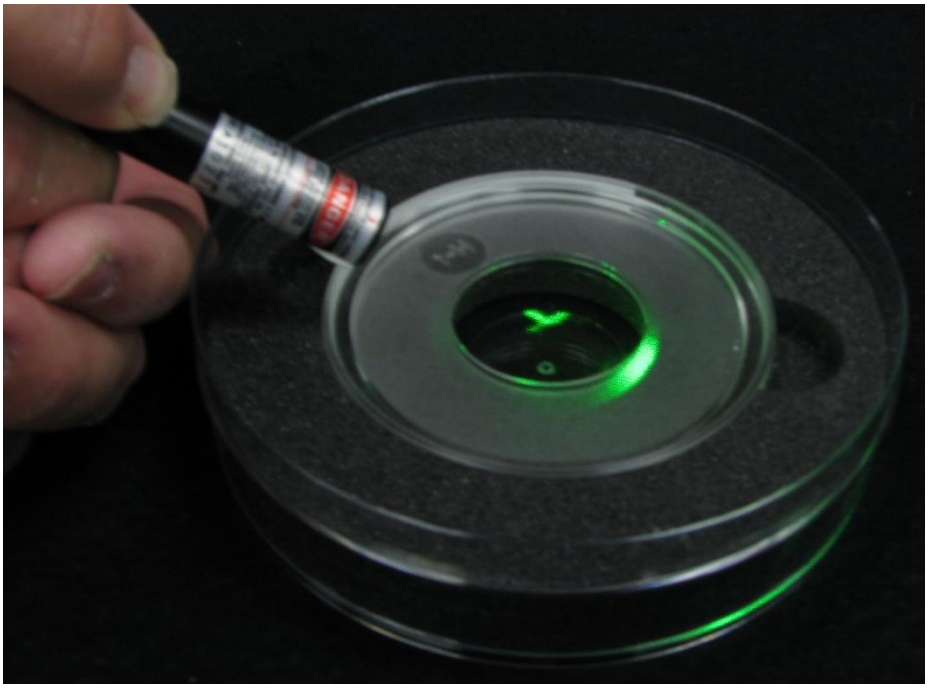

Figure 5. Hunter Lab haze standard illuminated by a green laser beam showing the volumetric scattering

3.2 Analysis

The laser used is a low-power (2–3 mW) red diode laser, and the scattered light from the haze standard is relatively small. In addition, our digital signal processing system measures a small signal from the room lights, so it is important to subtract an offset from the measured signals. We will take readings from the two detectors with the laser off, $h_{s,1,off}$ and $h_{s,2,off}$, and then take readings when the laser is turned on, $h_{s,1,on}$ and $h_{s,2,on}$. Subtracting these yields the measured signals corresponding to the light scattered by the haze standard.

$$h_{s,1} = h_{s,1,on} - h_{s,1,off} \quad \text{and} \quad h_{s,2} = h_{s,2,on} - h_{s,2,off}$$

Measurement 1 is from a detector at a small angle relative to the laser beam, in our case 14 degrees, while measurement 2 is from a detector at higher angle, in our case 42 degrees. We would like to correlate these two measurements to the ASTM haze measurement. We start by assuming that the scattered light is cylindrically symmetric and then calculate a solid angle associated with each detector. The ASTM haze measurement captures scattered light from 2.5 degrees to 90 degrees from the light beam. We assume that our 14-degree detector is a representative average of this scatter from 2.5 degrees to 28 degrees (the average of 14 and 42) and that the 42-degree sensor is a representative average from 28 degrees to 90 degrees. The solid-angle calculations show that detector 1 corresponds to 0.73 steradians and detector 2 corresponds to 6.3 steradians. Next, we note that in our current system, detector 2 is 29 inches from the scattering site and detector 1 is 33 inches away. Since the scattering site is small compared to these distances, the radiation seen by the detectors drops as 1 divided by the distance squared. So the signal from detector 1 must be multiplied by 1.3 so it can be compared to the signal from detector 2.

The haze standard is placed into the system and the scattering is measured by the two detectors. The haze standard is calibrated to have a haze of 0.85%, so we obtain the relation

$$0.85 = H(1.3*0.73*h_{s,1} + 1.0*6.3*h_{s,2})$$

from which we can find H. Replacing the haze standard with a windowpane, we again measure the scatter with the two detectors to obtain $h_{P,1}$ and $h_{P,2}$. The haze from the windowpane, h_P, is then given by

$$h_P = \frac{(1.3*0.73*h_{P,1} + 1.0*6.3*h_{P,2})}{H} = 0.85\frac{(1.3*0.73*h_{P,1} + 1.0*6.3*h_{P,2})}{(1.3*0.73*h_{s,1} + 1.0*6.3*h_{s,2})}$$

Since the 0.85% reading has a ±0.26% 2σ range, assuming our measurements and measurement process do not add substantial error, the error in the result is

$$+/-0.26\frac{(1.3*0.73*h_{P,1} + 1.0*6.3*h_{P,2})}{(1.3*0.73*h_{s,1} + 1.0*6.3*h_{s,2})}$$

3.3 Measurement Example

It should be mentioned here that, because of system limitations, we have been forced to launch the laser beam at the haze standard at an angle of 17 degrees. Consequently, the haze standard may scatter about 4% more light (cosine of 17 degrees) because of an increased path length. We chose to ignore this error because it is relatively small and because the windowpane will also see an increased path length, so the effect is somewhat cancelled.

When we measured the scatter from the haze standard, we measured 5.75 mV with the 14-degree detector and 0.39 mV with the 42-degree detector (offsets have been removed; all readings are about ±0.01 mV). We then placed a plastic window into the system and (after cleaning the surfaces) we measured 2.72 mV at 14 degrees and 0.29 mV at 42 degrees.

The haze standard scatters more light at both angles than the plastic window, but the angular dependence of the scattering is different. Visually the haze standard is scattering mainly from its volume, whereas the plastic window is scattering more from its surfaces. The plastic window might have small surface scratches.

Putting these measured values into the expressions above we find that

$$(1.3*0.73*h_{s,1}+1.0*6.3*h_{s,2})=7.95 \quad \text{and} \quad (1.3*0.73*h_{P,1}+1.0*6.3*h_{P,2}) = 4.41$$

so the pane scatter h_P is 0.47±0.14 (2σ), indicating that this particular window has a better than 50% chance of having less than 0.5% scatter.

3.4 Hardware

Figure 6 shows the two haze receivers. Each is composed of a 1-inch-diameter, 2-inch-focal-length glass lens that collects and focuses light from the scattering site onto a large-area detector.

Figure 6. Two haze receivers, composed of a lens and large-area photodetector

Figure 7 shows the laser and the aperture. The aperture is ¼ inch in diameter and is located 20 inches from the laser. The laser beam has been focused so that it is a small point at the aperture, passing through the aperture with minimal loss. The purpose of the aperture is to block stray light emerging from the laser, in order to prevent it from hitting the haze standard. The distance from the aperture to the haze standard is about 40 inches, so the spot on the haze standard is smaller than the roughly 1⅝-inch clear region on the standard.

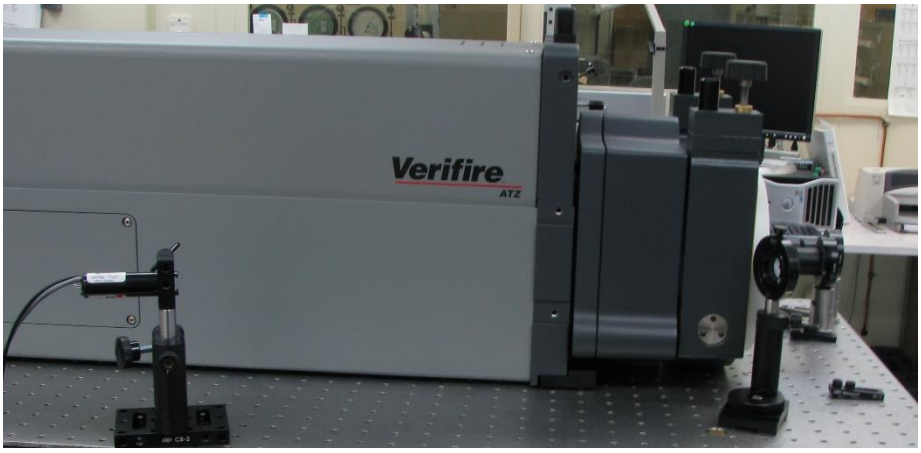

Figure 7. Laser used as the haze light source followed by an aperture to prevent stray light from interfering with the haze measurement

4 WEDGE

Sections 3.5.6 and 4.5.6 of JSC 66320, Revision A, provide the requirement that "The wedge of a category B plastic windowpane shall be less than or equal to 11 arc minutes in any direction" and the verification statement, "This requirement shall be verified by acceptance test and analysis." In addition, the verification section, 4.5.6, states that "The wedge orientation shall be marked on each pane in an inconspicuous area such as on the edge of the pane or within 13 mm (~0.5 in) of the perimeter of the clear viewing area. The individual windowpanes shall be assembled and positioned in the frame for a window assembly such that line of sight deviation is minimized wherever possible."

4.1 Discussion

A *wedge* is defined in the requirements document as "the angle formed by and between the two surfaces of an individual windowpane." If the surfaces are flat this definition is acceptable, but if the surfaces are modulated then it isn't clear whether this definition refers to the surfaces formed by laying a flat surface on each side of the window (i.e., touching the three highest points on the window) or to a tip/tilt measurement as provided by a Zernike-type decomposition of the window's surface. We will assume the second definition.

The wedge limitations shown in Table 3-4 of JSC 66320 are large. For example, a 0.5 m diameter window with a 10 arcmin wedge and flat surfaces would have a 0.003 rad wedge and be 1.5 mm thicker on one edge than on the opposite edge. One might suggest simply using a micrometer and measuring around the edge of the window to determine the wedge angle, but we will not have access to the edge and do not want to touch the window. For this reason, we propose to use the Zygo Phase-Shifting Interferometer along with known adjustments to the reference mirror to measure the wedge angle.

Since the measurement requirement is ≤11 arcmin, we need to ensure that the measurement is accurate to ±0.5 arcmin. No angle tolerance is provided for the orientation measurement.

4.2 Measurement Approach

Assuming that the reference mirror on the Zygo interferometer has been carefully aligned (recall that this system is described in detail in NASA TM NESC-RP-14-00951, April 2016), there will be less than 1 fringe across the 6-inch reference mirror. This corresponds to a tilt of about half a wavelength (633 nm/2) across 6 inches (150 mm), or about 0.007 arcmin of tilt. Assuming that this is the measurement error, the Zygo interferometer has much better accuracy than required to make the wedge measurement.

Surprisingly, the Zygo interferometer can generate a wavefront even if the wedge angle is fairly large. Testing has confirmed that even if the peak-valley measurement across a wedge is 150 waves, the Zygo can produce a valid wavefront measurement. Since the wavelength is 633 nm, this corresponds to a path length difference of about 95 microns across the 150 mm aperture of the system. This corresponds to a mirror tilt angle of 0.00063 rad or about 2.17 arcmin. If the index of refraction of the plastic window is 1.5, then this corresponds to a wedge angle of 1.44 arcmin.

If the wedge angle is more than about 1.5 arcmin, then the Zygo will not produce a waveform. One possible route to allow larger wedge angles to be measured would be to adjust the reference mirror by a known tilt in order to minimize or remove the effect of the wedge angle. Then the wedge angle and direction can be calculated from the tilt angle of the mirror. Both approaches are discussed in the following section; however, if a windowpane has such a large wedge that the reference mirror has to be adjusted, then it likely has additional surface variations and it may not be possible to obtain a valid tilt reading using the Zygo. In this case, the window will likely fail the wavefront criteria and the resultant wedge measurement may not be an issue.

4.3 Testing

When the Zygo makes a measurement of the optical path length through an object, the MetroPro software can be used to construct a Zernike polynomial decomposition of this measurement. For example, the text below has been taken from the Zernike decomposition performed by the MetroPro software on a test window. It shows the first four Zernike terms plus the rms of the remaining function. In this case the value −2.295 corresponds to the piston contribution (Z_0), which is just an overall offset in the dataset that can be ignored. The number −6.032 corresponds (Z_1) to the net tilt/tip about an axis situated vertically relative to the reference mirror, and the number 1.155 corresponds (Z_2) to the net tilt/tip about a horizontal axis lying in the plane of the reference mirror.

"Zernike Coefficients from”, 695471," data points"
"Order: Sphere"," Terms: “, 4,” rms: ", 2.475
−2.295, −6.032, 1.155, −0.463

There are differing formulas for the normalization of the Zernike polynomial coefficients, so in order to interpret the numbers provided by the MetroPro software, we adjusted the tilt angle of the reference mirror and tracked the peak-valley readings associated with these pure tip/tilt states with the Zernike polynomial decomposition. What we found was that the tip/tilt numbers correspond to one-half of the peak-valley reading in waves. In other words, if the mirror is tilted such that the difference in distance to the interferometer on one side of the mirror is ten waves

more than on the opposing side of the mirror, then the corresponding Zernike polynomial coefficient will be ±5. We verified this ratio out to a 150-wave difference in both tilt and tip. We also used a laser to ensure that we understood the sign convention used by the Zygo system. We added small notes to the reference mirror mount, stating the correspondence between negative Zernike coefficients to the side of the mirror with the larger wedge distance.

Summarizing, the horizontal and vertical components of the wedge angle can be found from the Zernike decomposition values, using

$$\theta_{x,y}(\text{min}) = \frac{2(Z_{1,2})0.633}{150*10^3}\frac{180}{3.14}\frac{60}{n}$$

where n is the index of the plastic windowpane. These two angles can be found from each Zygo 150 mm diameter scan and can be averaged to yield total tilts in the horizontal and vertical directions. Section 4.4, Data Analysis, describes how to convert these to a total wedge angle amount and direction.

To allow for a wedge angle greater than 1.5 arcmin, two micrometers were installed in the reference mirror 5-axis adjustment holder so that each tilt angle adjustment could be quantified (see Figure 8). Then, a laser beam was bounced off the front face of the reference mirror and focused onto a spot 272 inches from the reference mirror. Adjusting either micrometer by 400 µm caused the spot to move about 0.97 inches (left-right or up-down). That's about 12.27 arcmin of total angular deflection, which means the window has tilted by 6.13 arcmin, or about 0.0153 arcmin per micron adjustment. The micrometers used have 10 µm markings and a backlash of about 10 µm, so the precision and error in this measurement is about 0.15 arcmin.

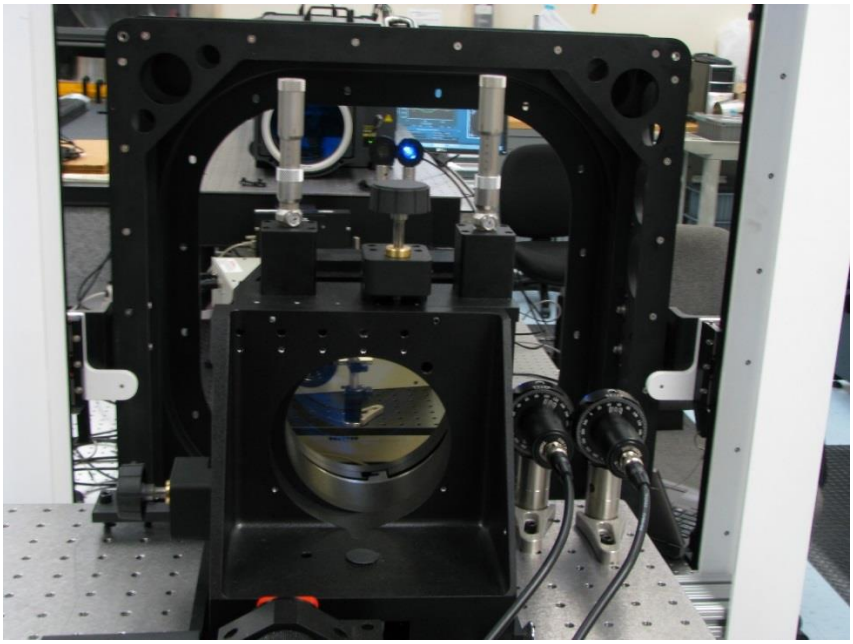

Figure 8. Reference mirror for Zygo interferometer with two micrometers attached in order to quantify the angular deviation of the mirror

We then aligned the reference mirror to yield less than 1 fringe on the Zygo interferometer wavefront measurement and turned one of the micrometers by 30 μm (about 0.46 arcmin) to see what measurement the Zygo interferometer provided. The screen showed 50 fringes across 145 mm (the aperture was reduced in this measurement from the maximum of 152 mm). The 50 fringes corresponds to a path difference of 25 wavelengths across the viewing area, or about 15.8 μm. The MetroPro software showed about 16 μm of path difference, indicating good agreement between the visual image and the Zygo analysis. The corresponding angle is then 0.38 arcmin. This is about 0.08 arcmin smaller than expected, but within the 0.15 arcmin error caused by backlash in the micrometers, so it is a reasonable result.

4.4 Data Analysis

The Zygo interferometer can only monitor 6-inch-diameter subapertures of the windowpane. Consequently, we will use the X-Y scanner to perform measurements over a majority of the window area, taking care not to overlap subaperture measurement areas too much. We will obtain Cartesian component tilt values, i.e., tip and tilt. These can be found from the Zygo data or from the micrometer readings. These angles can be averaged to obtain averaged *x* and *y* wedge angles for the pane. Then these Cartesian angles can converted to a total tilt angle and orientation as follows:

a. Let *a* and *b* be the average *x* and *y* wedge angles.

b. The parameters *a* and *b* in radians correspond, in the small angle limit, to slopes and describe the equation for a plane given by $z = ax + by$.

c. The gradient of this function is the vector $\nabla z = (a, b)$, which represents the direction and magnitude of the greatest slope of the plane.

d. The wedge orientation is then given by $\mathrm{Arctan}[b/a]$ (measured from the *x*-axis and accounting for sign ambiguities) and the magnitude of the wedge angle is given by $\sqrt{a^2 + b^2}$.

Wedge direction is measured from the "Positive X-Axis," which is the right "half" of the horizontal axis that passes through the center of the Zygo mirror, when facing into the interferometer aperture. Positive angle is measured CW from this orientation.

Since the angles are accurate to within 0.15 arcmin, the total angle magnitude will be accurate to better than ±0.5 arcmin as required. Note that the error in the orientation can be very large if the wedge angles are very small, so we simply state that for moderate wedge angles, the orientation angle should be reasonably well determined, but that for small wedge angles, where the wedge is not significant, the orientation angle may not be determinable.

5 BIREFRINGENCE

Sections 3.5.7.1 and 4.5.7.1 of JSC 66320, Revision A, provide the requirement that "The birefringence shall be less than 12 nanometers of retardance per centimeter of windowpane thickness over visible wavelengths of 450 nm to 650 nm" and the verification statements, "This requirement shall be verified by acceptance test and analysis of each windowpane" and "The birefringence, effective optical retardance values, shall be measured over a grid of measurement

points extending across the clear viewing aperture of the windowpane, to within 2.54 cm (1.0 inch) of the edge of the aperture. The measurement grid spacing shall not exceed 1.0 cm (0.39 inches) in any direction. The birefringence shall be computed at each measurement location."

5.1 Discussion

If, for example, a window has a clear viewing area of about 30 × 30 cm (about 1 square foot) then it will require measurements over a region 25 × 25 cm, i.e., $26^2 = 676$ measurements. If we have to make a manual adjustment at every measurement, this will take a very long time. Therefore we want a measurement approach that requires no adjustments so that it can be installed in a scanning system and used to automatically make the desired measurements. The analysis and measurement procedure described below provides this capability.

The wording of the requirement indicates that measurements are necessary across the entire 450–650 nm band, but this seems excessive. We questioned this and were told that it is sufficient to make a birefringence measurement at a single wavelength (or small band of wavelengths) within the 450–650 nm visible band. As will be shown in the next section, the effect of birefringence is magnified toward the blue end of the spectrum, so we will work at that end of the 450–650 nm band.

In general, any location on the pane has a pair of eigen-polarizations that pass through unchanged. The retardance is the effective index difference between these two modes. However, measuring this retardance in an automatic fashion over a window would be difficult and a simplifying assumption is needed. Our measurements on higher-quality sample windows and our discussions have indicated that the eigen-polarizations can be assumed to be linear. Making this assumption greatly simplifies the measurement (as opposed to having to search for elliptical eigen-polarizations) and allows an automatic measurement approach to be used.

5.2 Analysis

The requirement states that the retardance between two linear eigen-polarizations must be less than 12 nm/cm, i.e.,

$$n_s d - n_f d < 1.2\times10^{-6} d$$

where d is the thickness of the pane and n_s and n_f are the indices of the slow and fast eigen-polarizations in the pane. Dividing out the distance, the requirement becomes

$$n_s - n_f < 12 \text{ nm/cm} = 1.2\times10^{-6}$$

The easiest way to measure such a small difference in index is to instead measure the relative phase difference, $\phi_s - \phi_f$, between light traveling through each eigen-polarization. The relationship between these is given by

$$\phi_s - \phi_f = \frac{2\pi d}{\lambda}(n_s - n_f)$$

where λ is the vacuum wavelength of the light. Note that the largest phase difference occurs for the shortest wavelength of light, so we will aim to make our measurements with light near the 450 nm end of the spectrum. We chose to use 470 nm LEDs to make the measurements.

The measurement plan is to launch polarized light through the pane and to measure the amount of that light that passes through a crossed polarizer, then launch a second beam of polarized light, at 45 degrees to the first polarized beam, through the pane and measure how much of that gets through a crossed polarizer. We will show that if these two signals are normalized and then added together and if the polarizer performance is known, then the phase difference between the eigen-polarizations can be found regardless of the orientation of the pane birefringent axes.

Step A:

We start by assuming the existence of a beam of unpolarized light, i.e., broadband light where the electric field at any point in space is rapidly changing in magnitude and direction. Mathematically, this light can be represented as

$$\vec{l} = \begin{pmatrix} a \\ a\,e^{i\varphi} \end{pmatrix}$$

where a is the amplitude of the light along each Cartesian axis (chosen arbitrarily perpendicular to the direction of motion of the light) and φ is a random phase that is uniformly distributed between 0 and 2π radians.

Recall that a photodetector measures the time-averaged intensity of each polarization state and adds them together, sampling all values of φ in the process. So if a photodetector measures the intensity of this beam, it will yield

$$I_D = \frac{1}{2\pi}\int_0^{2\pi} \vec{l}\,\vec{l}^{\,*}\,d\varphi = 2a^2$$

So $2a^2$ is the intensity of the beam of light.

Step B:

Now choose a polarizer $P(\eta)$, which can be rotated by angle η. It can be represented by the following matrix

$$P(0) = \begin{pmatrix} t & 0 \\ 0 & r \end{pmatrix}$$

where t is the transmitted polarization throughput (t is close to 1 in value) and r is the rejected polarization throughput (r is close to 0 in value). We have chosen the axes such that $\eta = 0$ corresponds to having the transmitted polarization axis aligned with the first Cartesian axis as shown in the matrix.

If the polarizer is placed between the light source and the detector, the detector will measure a signal given by

$$I_D = \frac{1}{2\pi}\int_0^{2\pi} (P(0)\vec{l})(P(0)\vec{l})^* d\varphi = a^2(r^2 + t^2)$$

If two coaligned polarizers are placed between the light source and the detector, the detector will measure a signal given by

$$I_D = \frac{1}{2\pi}\int_0^{2\pi} (P(0)P(0)\vec{l})(P(0)P(0)\vec{l})^* d\varphi = a^2(r^4 + t^4) \approx a^2 t^4$$

Step C:

Now introduce a rotation matrix $R(\theta)$, given by

$$R(\theta) = \begin{pmatrix} \cos\theta & -\sin\theta \\ \sin\theta & \cos\theta \end{pmatrix}$$

Using this, we can find the matrix representing a polarizer rotated by 90 degrees, $P(90)$,

$$P(90) = R(90)P(0)R(-90) = \begin{pmatrix} r & 0 \\ 0 & t \end{pmatrix}$$

If a pair of crossed polarizers are placed between the light source and the detector, the detector will measure a signal given by

$$I_D = \frac{1}{2\pi}\int_0^{2\pi} (P(90)P(0)\vec{l})(P(90)P(0)\vec{l})^* d\varphi = 2a^2 r^2 t^2$$

Using the above equations, it is possible to find values for t and r for a given polarizer, as well as the value of a.

Step D:

The plastic pane can be modeled as having two linear eigen-polarizations with phase delays given by ϕ_s and ϕ_f and that are rotated by some angle θ, relative to the Cartesian axes defined by the polarizers. The Jones matrix for this pane, $W(\phi_s, \phi_f, \theta)$, is then given by

$$W(\phi_s, \phi_f, \theta) = \tau R(\theta)\begin{pmatrix} e^{i\phi_s} & 0 \\ 0 & e^{i\phi_f} \end{pmatrix} R(-\theta) = \tau\begin{pmatrix} e^{i\phi_s}\cos^2\theta + e^{i\phi_f}\sin^2\theta & (e^{i\phi_s} - e^{i\phi_f})\cos\theta\sin\theta \\ (e^{i\phi_s} - e^{i\phi_f})\cos\theta\sin\theta & e^{i\phi_f}\cos^2\theta + e^{i\phi_s}\sin^2\theta \end{pmatrix}$$

where τ is the amplitude transmission of the pane at the wavelength generated by the light source.

If this pane is placed between the light source and the detector, then the detector will measure a signal given by

$$I_D = \frac{1}{2\pi}\int_0^{2\pi} (W(\phi_s,\phi_f,\theta)\vec{l})(W(\phi_s,\phi_f,\theta)\vec{l})^* d\varphi = 2a^2\tau^2$$

Comparing this to the signal seen with nothing between the light source and the detector, i.e., where the detector sees a signal given by $2a^2$, it is seen that τ^2 is the intensity transmission of the pane.

Step E:

Now, place the pane between two crossed polarizers and place that between the light source and the detector. The detector will produce a signal given by

$$I_D = \frac{1}{2\pi}\int_0^{2\pi} (P(90)W(\phi_s,\phi_f,\theta)P(0)\vec{l})(P(90)W(\phi_s,\phi_f,\theta)P(0)\vec{l})^* d\varphi$$
$$= \frac{a^2\tau^2}{4}(r^4 + 6r^2t^2 + t^4 + (r-t)^2(r+t)^2(-\cos(4\theta) - (1-\cos(4\theta))\cos(\phi_s - \phi_f)))$$

Now, rotate the two polarizers by 45 degrees and take a second reading from the detector:

$$I_D = \frac{1}{2\pi}\int_0^{2\pi} (P(45)W(\phi_s,\phi_f,\theta)P(-45)\vec{l})(P(45)W(\phi_s,\phi_f,\theta)P(-45)\vec{l})^* d\varphi$$
$$= \frac{a^2\tau^2}{4}(r^4 + 6r^2t^2 + t^4 + (r-t)^2(r+t)^2(\cos(4\theta) - (\cos(4\theta)+1)\cos(\phi_s - \phi_f)))$$

If we add these two signals, we obtain

$$\frac{a^2\tau^2}{2}(r^4 + 6r^2t^2 + t^4 - (r-t)^2(r+t)^2\cos(\phi_s - \phi_f))$$

from which we can find the phase difference $\phi_s - \phi_f$. Note that if the phase difference is zero, then this becomes

$$4a^2\tau^2r^2t^2$$

which is equal to twice the crossed polarizer result with the pane loss added. This makes sense since two signals were added to obtain this result. Also, there is a 2π ambiguity in the phase determination. We assume that the windows under evaluation have retardance values small enough that this will not be a concern and that only the smallest calculated phase difference is appropriate.

Step F:

In practice, we need to automate the process so we will have two sets of crossed polarizers. Assuming that the polarizers used are identical in performance, but that the amount of light detected might be different for each polarizer pair, we will then need to measure a_1 and a_2, the amplitudes for each polarizer pair, separately.

The best way to do this is to rotate the polarizers into a parallel state to obtain the most light/signal and then to use

$$I_D = \frac{1}{2\pi}\int_0^{2\pi} (P(0)P(0)\vec{l})(P(0)P(0)\vec{l})^* d\varphi = a_{1,2}{}^2(r^4 + t^4) \approx a_{1,2}{}^2 t^4$$

where we know t, and will find the amplitudes (a_1 and a_2). Now, as the pane is scanned and we obtain the following two measurements,

$$I_{D,1} = \frac{1}{2\pi}\int_0^{2\pi} (P(90)W(\phi_s,\phi_f,\theta)P(0)\vec{l})(P(90)W(\phi_s,\phi_f,\theta)P(0)\vec{l})^* d\varphi$$
$$= \frac{a_1{}^2\tau^2}{4}(r^4 + 6r^2t^2 + t^4 + (r-t)^2(r+t)^2(-\cos(4\theta) - (1-\cos(4\theta))\cos(\phi_s - \phi_f)))$$

$$I_{D,2} = \frac{1}{2\pi}\int_0^{2\pi} (P(45)W(\phi_s,\phi_f,\theta)P(-45)\vec{l})(P(45)W(\phi_s,\phi_f,\theta)P(-45)\vec{l})^* d\varphi$$
$$= \frac{a_2{}^2\tau^2}{4}(r^4 + 6r^2t^2 + t^4 + (r-t)^2(r+t)^2(\cos(4\theta) - (\cos(4\theta)+1)\cos(\phi_s - \phi_f)))$$

we can divide $I_{D,1}$ by a_1 and $I_{D,2}$ by a_2, and then add the results to find the phase difference.

5.3 Hardware

As shown in Figure 9, the measurement system is composed of a pair of polarized 470 nm LED transmitters and a pair of polarized receivers. (Photos of the hardware are shown in Section 9.) The LED transmitters contain 1-inch-diameter, 2-inch-focal-length lenses in order to direct more light toward the receivers, but care has been taken not to focus this light. The lenses are used only to increase the light level and not to produce structured light that might vary because of an unwanted effect such as beam steering. For this reason, the lenses are closer than 2 inches to the LEDs, such that they will not produce an image of the LEDs emission in the far field.

The polarizers in both the transmitters and in the receivers were cut from high-contrast linear polarizing film purchased from Edmund Optics, with a published single transmission of 42%, parallel 36%, and crossed <0.004% (9000:1 extinction ratio). We measured a single transmission of 41.38%, a parallel transmission of 34.23%, and a crossed transmission of 0.0155% (2208:1 transmission ratio as one of the polarizers is rotated). These numbers are not the same as those provided by the vendor; however, these films work optimally at wavelengths longer than

470 nm. There might be an advantage to shifting the measurement to the red portion of the spectrum, but we have not analyzed this to determine if that is the case or not. Using these measurements and the equations in the Analysis section (5.2), we obtained the values $t = 0.9096$ and $r = 0.01369$ for the polarizing film.

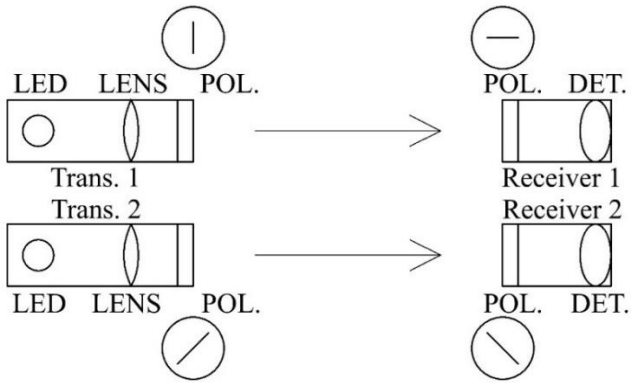

Figure 9. Birefringence measurement system

Recall that one of the LEDs is driven at 200 Hz and one at 250 Hz in order for their signals to be separated by our digital signal processing routine.

The two transmitter/receiver pairs are physically spaced by 4 cm horizontally and 3 cm vertically (see the photos in Section 9). So as the mounted windowpane is scanned, the reading from one pair is looking through a portion of the window shifted horizontally and vertically from the second pair. The data from each pair is saved and assigned to a location so that the two measurements through the same portion of the window can be merged after the scan and processed to yield the retardance.

5.4 Measurements

Before the system can be used, the values for a_1 and a_2 must be found. The process below describes how this is done and, as an added benefit, it ensures that the polarizers are in the correct orientation to perform the measurements.

a. Start by turning on only the first transmitter/receiver pair and align the polarizers approximately parallel in order to obtain a large signal, well above the offset/noise floor.

b. *Optional*: Take a sheet of polarizing film with known polarization axes and place it between the transmitter and the receiver with the polarization axis either horizontal or vertical to the table, whichever produces the smallest signal. Now rotate the transmitter polarizer to obtain the smallest possible signal. Lock down the transmitter polarizer, which is now in a horizontal/vertical orientation and remove the sheet polarizer.

c. If step b was skipped, lock down the transmitter polarizer so it is fixed.

d. Rotate the receiver polarizer until a minimal signal is obtained, i.e., crossed polarizers. Note the rotation angle at which this occurs.

e. Rotate the receiver polarizer 90 degrees, which should produce a maximal signal. Using this voltage reading, a_1 can be found.

f. Rotate the receiver polarizer back 90 degrees, which should yield a minimal signal, and lock it in place.

g. Keeping the first transmitter turned on, adjust the polarizer on the second receiver until the signal it is picking up from the first polarizer is minimal (i.e., crossed polarizers).

h. Now rotate the polarizer on the second receiver by 45 degrees and lock it in place.

i. Turn off the first source and turn on the second source.

j. Adjust the polarizer on the second source to yield a minimal signal and note this rotation angle.

k. Rotate the second source polarizer by 90 degrees, which should yield a maximal signal, and use this reading to obtain a_2.

l. Rotate the second source polarizer back to the minimal signal position and lock the polarizer in place.

After following the above procedure, the system is set up and birefringence values can be measured. We did this and obtained values for a_1^2 and a_2^2 on a lab bench setup of 945 mV and 1408 mV, respectively. There were about 100 μV of crosstalk between the two transmitter/ receiver pairs, which is negligible. The signal levels with no window present were about 800–900 μV because of the small amount of light that made it through the crossed polarizers at 470 nm. Placing a plastic window into the system, we measured 1.33 mV on the first channel and 138.1 mV on the second channel. Dividing these by the corresponding a^2 value yields 0.00141 and 0.0981. Adding these and solving for the phase shift yields 46 degrees (0.8 radians). The plastic window was 0.5 inch thick, so this corresponds to a retardance of 47 nm/cm.

We ran a Monte Carlo analysis on the retardance measurement approach in order to obtain insight into the accuracy of the measurements. We assumed that the angle of a polarizer could be set to an accuracy of 1 degree and that the angle of a cross polarizer could be set to an accuracy of 0.5 degrees. We then ran a large number of simulations, varying the magnitude and the axis orientation of the windowpane birefringence, to obtain the results shown in Figure 10. Recall that the retardance requirement is 12 nm/cm, so based on our error discussion in Section 2, note “e,” we desire a measurement standard deviation of 0.25. Figure 10 shows that we are typically higher than this value for large values of retardance, and for small values of retardance, our standard deviation is roughly 0.75, which is three times the goal. If we need higher accuracy in the measurement, we can upgrade the polarizer rotation mounts in the future.

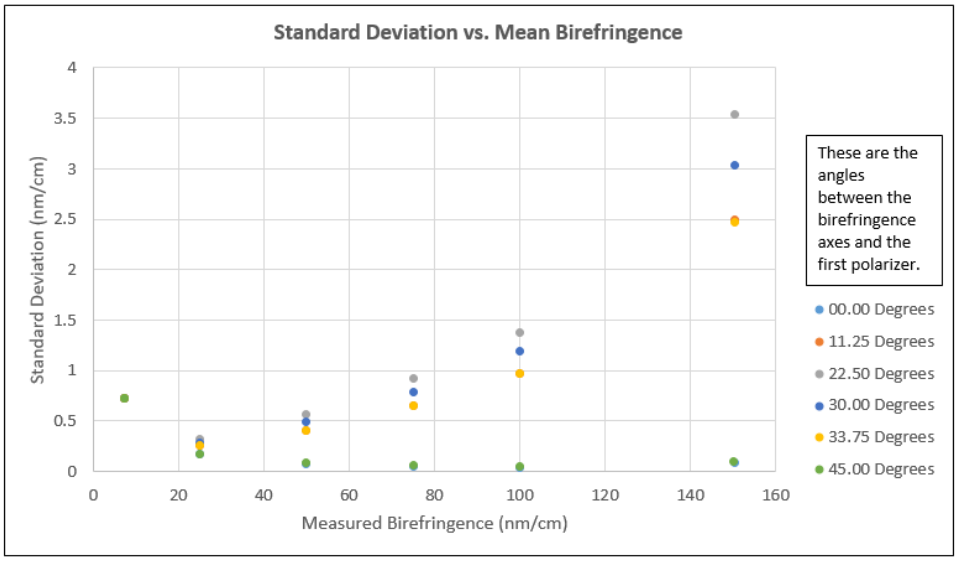

Figure 10. Calculated standard deviations in the retardance as a function of the pane birefringence magnitude and angle

6 SPECULAR REFLECTANCE

Sections 3.5.8 and 4.5.8 of JSC 66320, Revision A, provide the requirement that "Specular reflectance of normally incident light (minimum rms wavefront error) between 450 and 800 nanometers from each coated window surface shall not exceed 2% absolute (based on the integration of photon flux over the 450–800 spectral range)" and the verification statement, "This requirement shall be verified by qualification test and analysis. Reflectance shall be measured in 5 nm increments over the specified spectral range. Specular Reflectance may be verified in accordance with NIST Special Publication 250-48, *Spectral Reflectance.*"

6.1 Discussion

We had a concern with this requirement because measuring the reflectance of normally incident light is difficult. Even the reference instrument cited in NIST SP 250-48 is limited to measurement at angles larger than 5 degrees so that the reflected beam optics do not interfere with the incoming beam optics. However, in the present case the situation is more complicated because there are reflections from both the front and the back surfaces of the windowpane and they need to be separated such that the first surface reflection measurement is not affected by the second surface reflection. For this reason, we proposed to perform the reflection measurement at a small angle and showed analytically that, for a typical air/material interface, this would not affect the results significantly.

We constructed reflectance equipment and measured the reflectance of a plastic window sample, finding to our surprise that the reflected power oscillated with wavelength. We soon realized that the windowpane was coated (we believe this was an antiscratch coating) and that the reflections between the air and coating were coherently interfering with the reflections between the coating and the underlying plastic. We took more measurements and found that the reflectivity varied with location as well, probably because this interference effect is a strong function of the coating thickness, which may vary slightly with location on the window.

Having demonstrated that reflectance measurements varied with both angle and location on the window, we suggested that instead of measuring reflectance in a manner that would introduce error, we would calculate reflectance from the transmission data. The transmission data is taken in 5 nm steps from 380 to 800 nm. If the transmission values from 450 to 800 nm are all close to the theoretical values for a lossless material with two air/material reflection interfaces, then we can assume minimal absorption loss in this region. So a reasonable upper bound on the reflection in each 5 nm spectral band can be found by making two assumptions: (1) that all of the power lost in transmission is a result of reflection and (2) that the two windowpane surfaces are the same. This allows the reflection spectrum, and then the integrated reflection, to be found from the transmission data.

One more point, the phrase "based on the integration of photon flux over the 450–800 spectral range" yields a nonstandard definition of averaged reflectance. There are more photons per watt at longer wavelengths than at shorter wavelengths. So if a window has more reflectance at longer wavelengths than at shorter wavelengths, the average reflectance based on photon flux will be larger than that based on wattage. The mathematical expressions are derived in the following sections and an example given.

6.2 Analysis

Assume that spectral transmission data $t(\lambda)$ is available. If it is assumed that the only loss mechanism in the windowpane is reflection loss at each of the two surfaces and that the reflection at each surface is the same and given by $r(\lambda)$, then, ignoring internal reflections,

$$t(\lambda) = (1 - r(\lambda))^2$$

Solving for the reflectivity, we obtain

$$r(\lambda) = 1 - t(\lambda)^{1/2}$$

If we choose to include the first roundtrip light (i.e., the light that passes through the first interface and bounces off the back interface, and then bounces off the first interface and passes through the second interface), we obtain

$$t(\lambda) = (1 - r(\lambda))^2 + r(\lambda)^2(1 - r(\lambda))^2 = (1 + r(\lambda)^2)(1 - r(\lambda))^2$$

Solving this equation for the reflectivity is cumbersome, and the question is, "Is it necessary?" Consider an example where the transmission through a window is 0.92. The first equation yields a reflectivity of 0.0408 and the second, 0.0417. Since the requirement only shows one digit, we assume measurements to an accuracy of ±0.05 are necessary. Since the second equation yields an offset of 0.0009, it is well below the required accuracy and can be ignored.

Assume $r(\lambda_i)$ is the reflectivity for each 5 nm wavelength band from 450 to 800. One way to calculate the total reflectivity r is to just average these 71 results:

$$r = (1/71)\sum_i r(\lambda_i)$$

However, the requirement calls for integrated photon flux. Let $I(\lambda_i)$ be the total intensity of light (watts) launched at the windowpane in each wavelength band. The photon flux $p(\lambda_i)$ (photons/second) in each spectral band is given by

$$p(\lambda_i) = I(\lambda_i)/(h\nu) = \lambda_i I(\lambda_i)/(hc)$$

where h is Plank's constant (6.626 x 10^{-34} J-s) and c is the speed of light (3.0 x 10^8 m/s). The total incoming photon flux p is given by

$$p = \sum_i p(\lambda_i) = \sum_i \lambda_i I(\lambda_i)/(hc)$$

The reflected photon flux spectrum $p_r(\lambda_i)$ is given by

$$p_r(\lambda_i) = \lambda_i r(\lambda_i) I(\lambda_i)/(hc)$$

The total reflected photon flux p_r is given by

$$p_r = \sum_i p_r(\lambda_i) = \sum_i \lambda_i r(\lambda_i) I(\lambda_i)/(hc)$$

So the integrated photon flux reflectivity r_P is given by

$$r_P = \frac{\sum_i \lambda_i r(\lambda_i) I(\lambda_i)/(hc)}{\sum_i \lambda_i I(\lambda_i)/(hc)} = \frac{\sum_i \lambda_i r(\lambda_i) I(\lambda_i)}{\sum_i \lambda_i I(\lambda_i)}$$

Of course this is intensity-dependent, which we doubt was the intent of the requirement, so assuming the light intensity is the same in each spectral band, this dependence can be removed, leaving

$$r_P = \frac{\sum_i \lambda_i r(\lambda_i)}{\sum_i \lambda_i}$$

which biases the reflectivity to the long wave region.

6.3 Example

Figure 11 shows a sample transmission spectra in 5 nm steps from 450 to 800 nm.

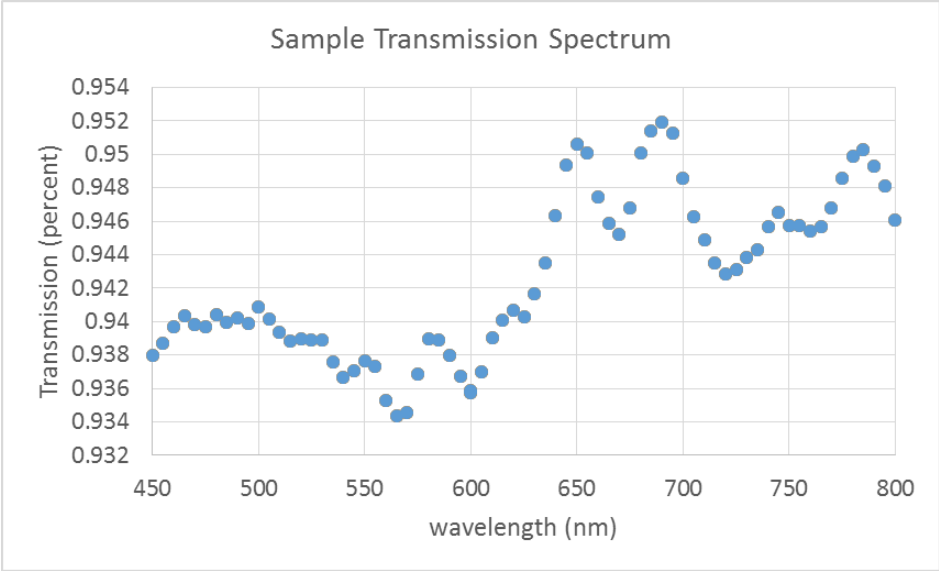

Figure 11. Sample transmission plot of a plastic window

Using the formula derived in Section 6.2, the reflectance spectra can be found and is shown in Figure 12.

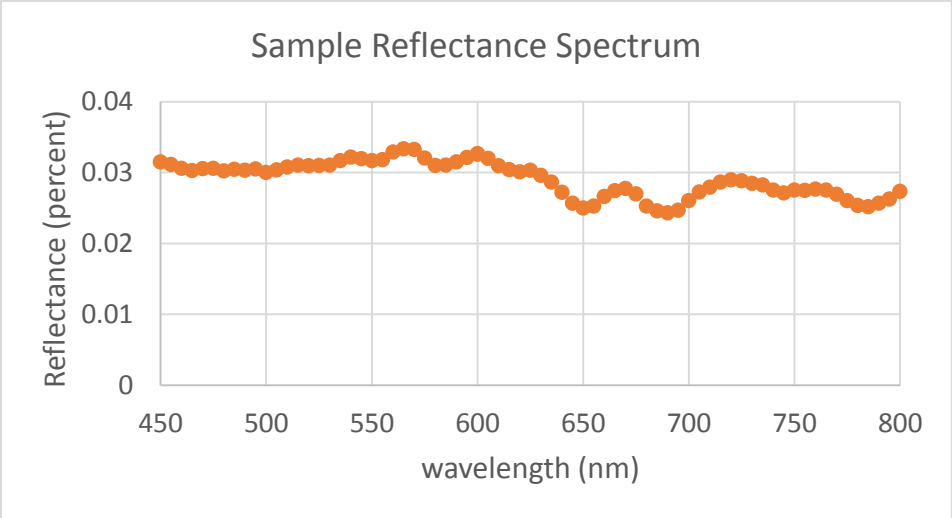

Figure 12. Reflectance spectrum corresponding to the transmission spectrum in Figure 11

The average reflectivity (which is the average of these reflection values) is 0.0291. The integrated photon flux reflectivity (given by the formula above) is 0.0288. The difference isn't significant in this case because the reflectivity doesn't change much with wavelength. So in either case, we would report the reflectivity as either 2.9% or just 3% along with the requested reflectance spectrum.

7 TRANSMITTANCE

Sections 3.5.9.1 and 4.5.9.1 of JSC 66320, Revision A, provide the requirement that "For individual glass windowpanes and category B plastic panes, the luminous transmittance shall be equal to or greater than 92% when coated or 90% when uncoated" and the verification statements, "Measurements shall be performed in accordance with ASTM D1003 or equivalent" and "Spectral transmittance data from 380–800 nanometers using a 5-nanometer wavelength resolution shall be provided to NASA in electronic format."

7.1 Discussion

The measurement approach described in ASTM D1003 states that "the specimen is placed against the entrance port of the integrating sphere," and we are reluctant to do this. The plastic panes being tested will be held in the framework shown earlier in this document, and this mounting is not completely rigid. The panes can move by a small amount, making it difficult to ensure that they will not impact the integrating sphere when it is brought very close to the pane.

We instead use a slightly modified version of the ASTM D1003 system to measure the transmission of the pane from 380 to 800 nm in 5 nm steps. We will then use CIE illuminant C and the 1931 tristimulus values, as called out in ASTM D1003, to calculate the luminous transmission. If the CIE illuminant values in 5 nm steps are given by $C(\lambda_i)$, the 1931 Y value tristimulus values are given by $\bar{y}(\lambda_i)$, and the transmission of the window by $t(\lambda_i)$, then the luminous transmission T is given by

$$T = \frac{\sum_i \bar{y}(\lambda_i) C(\lambda_i) t(\lambda_i)}{\sum_i \bar{y}(\lambda_i) C(\lambda_i)}$$

7.2 Measurement Approach/Hardware

The hardware used to measure transmittance is shown in Figure 13. The right side of the figure shows the light source in a blue box. This light is sent through a focusing lens, a chopper, and a filter wheel before impinging on the entrance slit to the monochromator. The entrance and exit slits are set to yield a 5 nm wide bandwidth for the light emerging from the monochromator, as determined by the grating dispersion. This light beam is collimated, launched through a region of space where the test pane will be located, and then focused onto a detector. A CaF2 window can be swung into the optical path so that its transmission can be measured.

In more detail, referring to Figure 13, the light source is a 20 W halogen bulb, typically operated a little below this level. It is designed for 12 V operation, and we typically operate it around 11.5 V. An aging bulb may provide a varying illumination; if the system noise begins to increase, it may mean that the bulb is nearing the end of its life. Also, we have noticed that new bulbs may require as much as a 24-hour burn-in before becoming stable. In addition, we typically turn on the bulb 2–3 hours before use so that it can come to thermal stability with its environment.

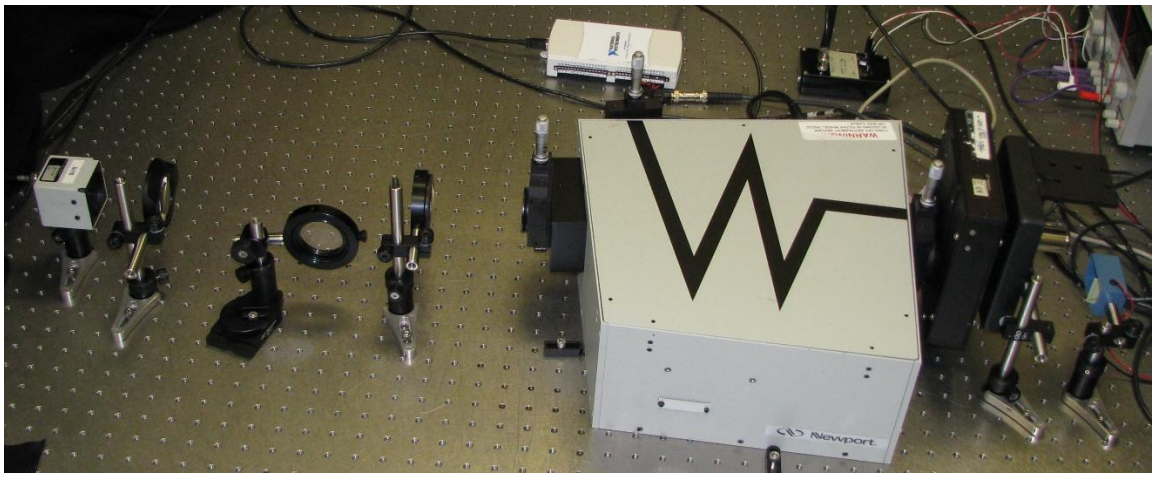

Figure 13. Transmission measurement system

A 1-inch-diameter lens with a 1-inch focal length is used to image the bulb filament onto the entrance slit of the monochromator. The slits are set to 0.77 mm, which corresponds to a 5 nm bandwidth. Before the light reaches the slit, it passes through a chopper wheel set to 200 Hz and then through a filter wheel (Figure 14). The filter wheel is under computer control and one of six filters can be selected. For the scan from 380 to 800 nm, we use two different filters. Recall that the purpose of the filters is to remove second order diffracted light from the grating so that it does not contaminate the primary diffracted light. For example, without the filters, 400 nm radiation can show up on the 800 nm setting. So we use a 325 nm long-pass filter from 380 to 600 nm and then a 450 nm long-pass filter from 600 to 800 nm.

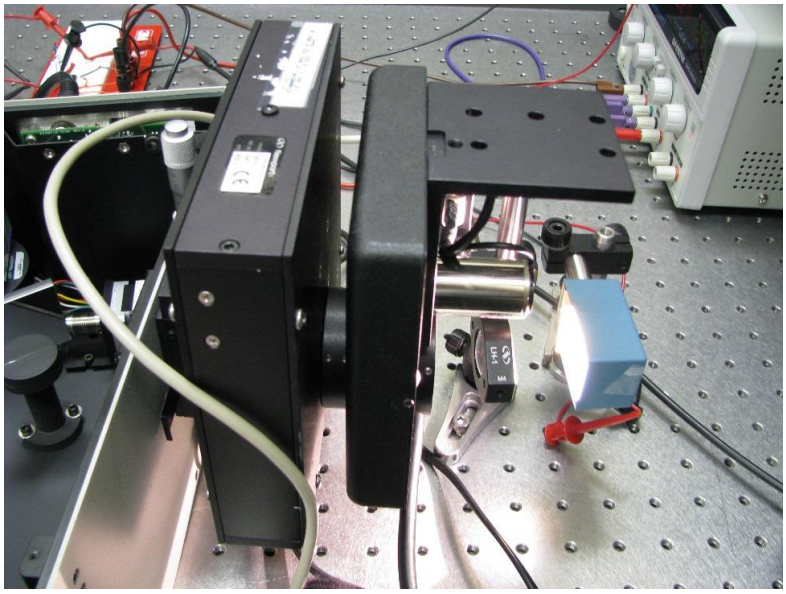

Figure 14. Light source, chopper, and filter wheel

Scattered light is a serious problem in performing spectroscopy measurements. We attempted to perform the transmission measurement with a compact Ocean Optics spectrometer and failed because of scattered light. Halogen bulb emission is high in the visible and near-infrared bands, and the detector is sensitive to this light. So when measurements are made in the short wave

380–450 nm range, where the halogen bulb has minimal emission and where the detector has relatively low responsivity, small amounts of bleedthrough of visible and near-infrared light can match or exceed the desired short wavelength signal. With our spectrometer, scattered light is greatly reduced when compared to a miniature spectrometer, but it is still a concern. In order to reduce it, we added a 650 short-pass filter to the 350 long-pass filter, so when this filter combination is in place, it blocks out waves shorter than 350 nm, preventing a possible second harmonic contamination. It also blocks light with wavelengths longer than 650 nm, i.e., most of the halogen bulb's emission (this bulb peaks around 900 nm), reducing the amount of unwanted radiation from entering the spectrometer and decreasing the scattered light.

The spectrometer uses a monochromator to disperse the incoming light into its spectral components. We chose to use a Newport Cornerstone 260 ¼ m monochromator for this purpose, shown in Figure 15 with the cover plate removed. The light enters from the right (through the entrance slit), reflects off a flat steering mirror, and then reaches a curved collimating mirror. The collimated light is directed toward a grating, which disperses the light into a rainbow pattern. This light reaches a focusing mirror that images the rainbow onto the exit slit.

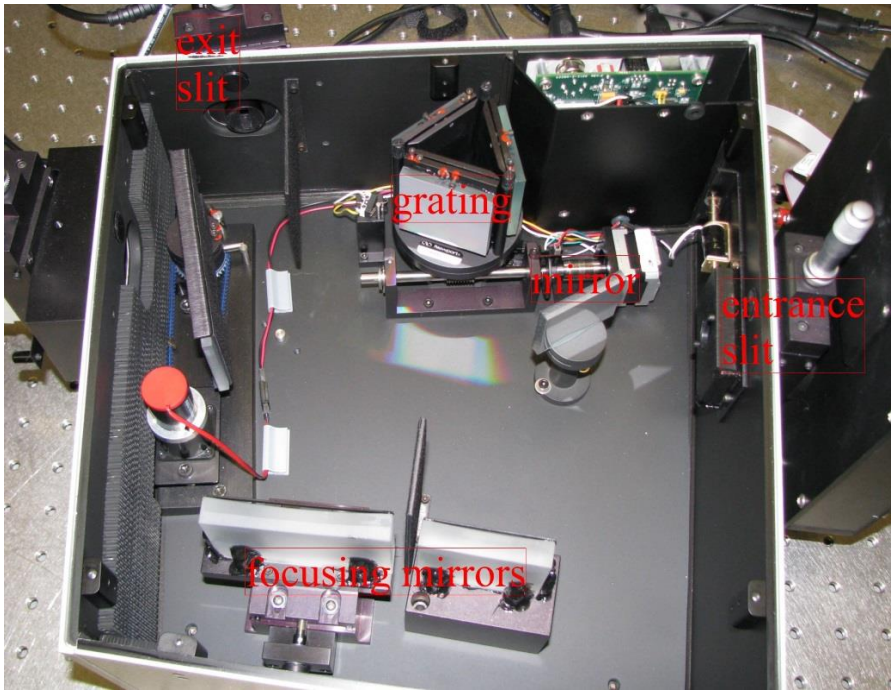

Figure 15. Interior optics of the Newport monochromator

The monochromator can select one of three gratings, to cover different spectral bands, but for the present purposes only one grating is needed. We use a Newport 74066 grating with 600 lines per millimeter. It has a primary wavelength region that reaches from 270 to 1000 nm, i.e., this is the region where the grating efficiency is greater than 20%. When used in this monochromator, this grating has an inverse dispersion of 6.5 nm/mm. So if we wish to operate in 5 nm bands, then the slit widths should be 0.77 mm; however, owing to diffraction effects, this width allows more than 5 nm throughput. We set the slits to 0.7 nm for performing 5 nm bandwidth scans (see Section 7.3, Testing).

When the light leaves the spectrometer, it is captured by an achromatic lens with a 150 mm focal length and roughly collimated as shown in Figure 16. The light reaches a second lens, which focuses it onto a large-area detector. In practice, the system is turned on and scanned without a window in order to obtain a reference scan. Next the window is put in place and a transmission scan made. Then the window is removed and a second reference scan taken to ensure that the system has not drifted during the measurement.

7.3 Testing

In order to verify the wavelength bandwidth and to verify that the monochromator is operating at the correct wavelengths, we used a 532 nm laser and a 632.8 nm laser, both narrowband light sources, as input sources for the spectrometer. In each case the slits were set to a 0.7 mm width, which should correspond to a bandwidth of a little less than 5 nm wavelength, but ends up slightly over, apparently as a result of diffraction effects. In both plots, it appears that the spectrometer is correctly calibrated to within 1 nm and has a bandwidth of a little over 5 nm, which is probably sufficient, so that when making 5 nm steps, nothing of interest is missed.

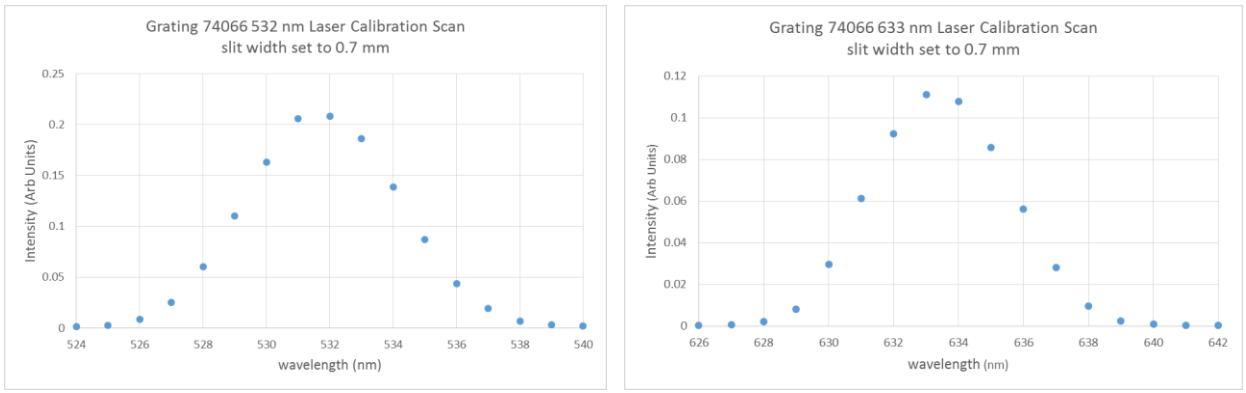

Figure 16. Output from the spectrometer when 532 and 632.8 nm laser sources are used, demonstrating that the spectrometer is wavelength-calibrated and that the slit widths yield the correct wavelength discrimination

We then set the spectrometer to scan from 300 to 800 nm in 5 nm steps and to switch filters at 600 nm. The goal was to measure the transmission of an uncoated CaF2 window, which should have good transmission through this range. As described above, we took a reference scan without the window, then one with the CaF2 window, and then a second scan without the window. We started each scan at 300 nm, below the cut-on of the 350 nm long-pass filter where there should be no light, in order to obtain an estimate of the scattered light. As shown in the plot in Figure 17, the flat area below about 360 nm produces a 0.0004 rms voltage offset to all of the data. This is not significant above 400 nm, but below 400 nm it is important. For consistency, we subtracted 0.0004 from all of the data from each run. Strictly speaking, this should not be done after the filter is changed, but it is such a small correction (in the 600–800 nm range) that it can be disregarded.

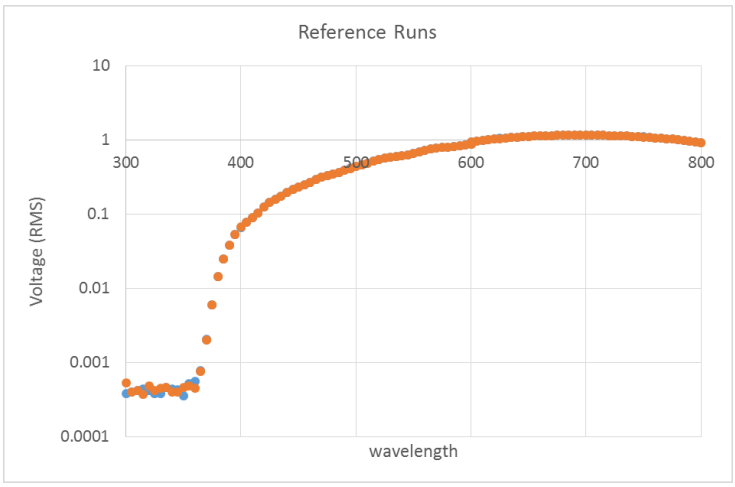

Figure 17. Two reference runs from 300 to 800 nm to show scattered light level on a log scale

The plot in Figure 18 shows the variation in the two reference runs as a percentage change. The errors are largest at short wavelengths where the signals are smallest, but overall the results are good and well within the tolerance needed to meet the requirement.

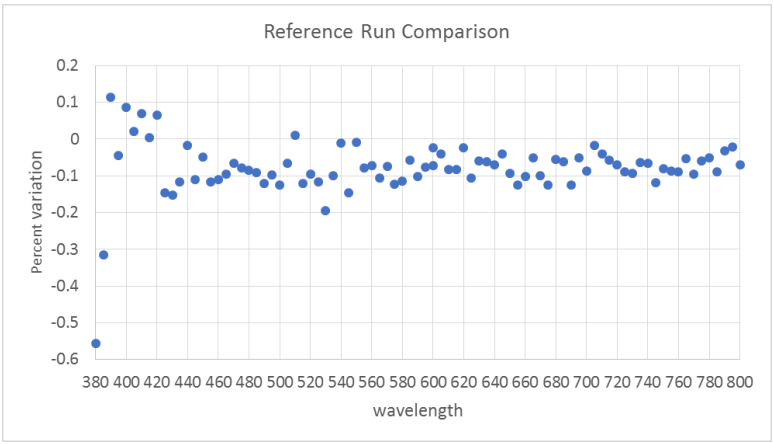

Figure 18. Comparison between reference runs from 380 to 800 nm

Then we scanned the CaF2 window from 300 to 800 nm. The result, which looks very similar to the reference runs, is shown in Figure 19 on a linear scale.

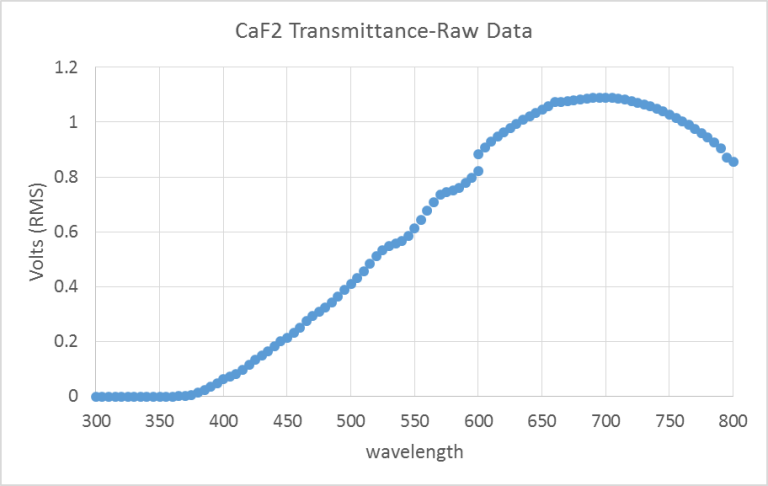

Figure 19. Raw transmission data for CaF2 window

Now, dividing the raw CaF2 data (with the offset subtracted) by each of the reference runs (with the offset subtracted) yields the plots shown in Figure 20. Note that the total vertical scale is only about 1%, demonstrating the quality of the data. The variations seen in the data are mostly about ±0.001 (±0.1%), which is adequate to meet the requirement. Also shown is the theoretical normal incidence transmission for a clean window of CaF2 based on an index of refraction determined from the Sellmeier equation (the blue dots). Above that (green dots) is the theoretical transmission for a clean window of CaF2, adding in the first recirculation of light between the window surfaces. The measured results are well in agreement with the theoretical prediction.

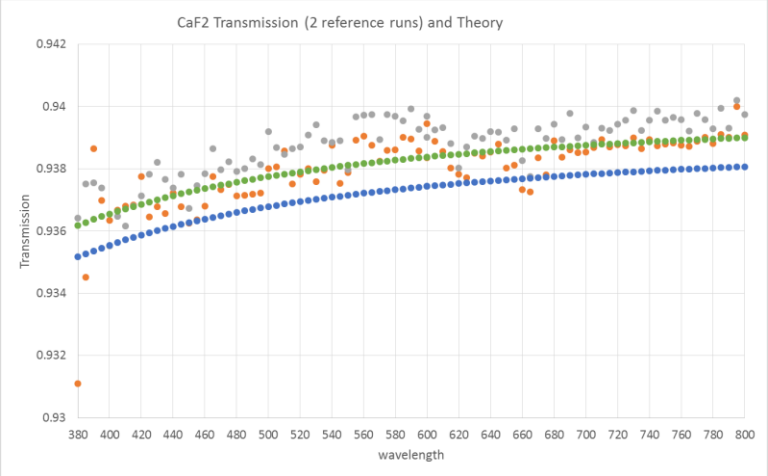

Figure 20. Measured transmission of CaF2 window versus wavelength using two different reference runs and compared with first- and second-order theory

The luminous transmission is heavily weighted to the 500–630 nm portion of the spectrum, so it is not surprising that the luminous transmission calculated for the example above is 0.939. The data below 450 nm plays only a small role in the luminous transmission, so the errors there are not significant in this calculation. However, the spectral transmission measurement is used to calculate the yellowness index (see Section 8), and in this calculation, small variations in the short wave region play a much larger role.

8 COLOR BALANCE/YELLOWNESS INDEX

Sections 3.5.10.2 and 4.5.10.2 of JSC 66320, Revision A, provide the requirement that "For plastic windowpanes, the yellowness index shall be less than 0.5" and the verification statement, "The contractor may use withdrawn standard ASTM D1925, *Test Method for Yellowness Index of Plastics*, as appropriate for the verification." We should mention that ASTM E313, *Standard Practice for Calculating Yellowness and Whiteness Indices from Instrumentally Measured Color Coordinates*, has been approved for use as well.

8.1 Discussion

ASTM E313 provides an expression for the yellowness index, but it assumes that the CIE tristimulus values are known. ASTM E313 cites several other ASTM documents from which we have selected ASTM E308, *Standard Practice for Computing the Colors of Objects by Using the CIE System*, to use to obtain the CIE tristimulus values. There are websites that supply versions of these tables, sometimes with more digits of resolution.

Note that ASTM E313 states that "For yellowness measurement, this practice is limited to specimens having dominant wavelength in the range 570 to 580 nm…" It might be argued that ASTM E313 is not the appropriate standard from which to measure the yellowness of highly transparent plastic panes. However, this is just an observation and does not affect the analysis approach described in Section 8.2.

8.2 Data Analysis

ASTM E313 states that the yellowness index (YI) is given by

$$YI = 100(C_X X - C_Z Z)/Y$$

where $X, Y,$ and Z are the measured tristimulus values of the specimen calculated for either Illuminate C or D_{65}, and either the CIE 1931 standard color-metric observer, or the CIE 1964 standard color-metric observer, and coefficients C_X and C_Z are selected from Table 1 for the selected illuminator and observer.

Table 1. Coefficients needed to calculate yellowness for the two standard sources, C and D65, and the two color-metric observer standards

	CIE Standard Illuminant and Standard Observer			
	C, 1931	D_{65}, 1931	C, 1964	D_{65}, 1964
C_X	1.2769	1.2985	1.2871	1.3013
C_Z	1.0592	1.1335	1.0781	1.1498

ASTM E308 defines the X, Y, Z tristimulus values as follows:

$$X = 100\frac{\sum_{\lambda} T(\lambda)S(\lambda)\bar{x}(\lambda)\Delta\lambda}{\sum_{\lambda} S(\lambda)\bar{y}(\lambda)\Delta\lambda}, \quad Y = 100\frac{\sum_{\lambda} T(\lambda)S(\lambda)\bar{y}(\lambda)\Delta\lambda}{\sum_{\lambda} S(\lambda)\bar{y}(\lambda)\Delta\lambda}, \quad Z = 100\frac{\sum_{\lambda} T(\lambda)S(\lambda)\bar{z}(\lambda)\Delta\lambda}{\sum_{\lambda} S(\lambda)\bar{y}(\lambda)\Delta\lambda}$$

$\bar{x}(\lambda)$, $\bar{y}(\lambda)$, and $\bar{z}(\lambda)$ are the spectral tristimulus values (color-matching functions) and are given in ASTM E308 in Table 1 for the CIE 1931 standard color-metric observer and in Table 2 for the CIE 1964 standard color-metric observer at 5 nm intervals from 380 to 780 nm. $S(\lambda)$ is the relative spectral power distribution and is given in ASTM E308 in Table 3 for CIE Illuminate C or D_{65} in 5 nm intervals from 380 to 780 nm. $T(\lambda)$ is the spectral transmission of the windowpane from 380 to 780 nm in 5 nm intervals. $\Delta\lambda$ is the wavelength spacing, which is assumed to be 5 nm.

Since there are two options for the standard observer and two options for the standard illumination, we propose to provide five values for the yellowness index, one for each option combination and an averaged value. Assuming no wavelength dependence on the transmission of a specimen, the yellowness figures for these five options are shown in Table 2. One might expect that the results would be zero, but the standard illuminants yield small yellowness offset values.

Table 2. Yellowness values for the two standard illuminations and the two standard observers

	CIE Standard Illuminant and Standard Observer				
	C, 1931	D_{65}, 1931	C, 1964	D_{65}, 1964	Average
YI	0.004	−0.002	−0.003	−0.027	−0.007

The three plots shown in Figure 21, Figure 22, and Figure 23 show the 1931 and 1964 tristimulus spectra and the spectra for the two standard illuminants, C and D65.

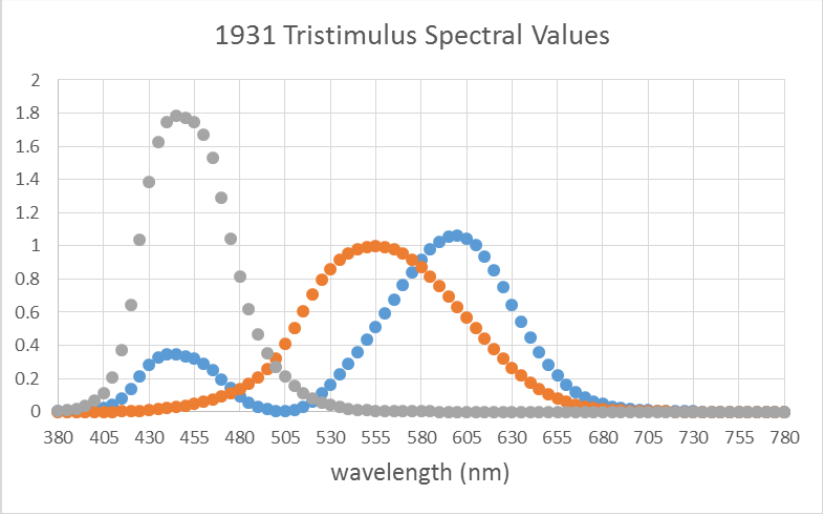

Figure 21. 1931 tristimulus spectral values (grey is Z, orange is Y, and blue is X)

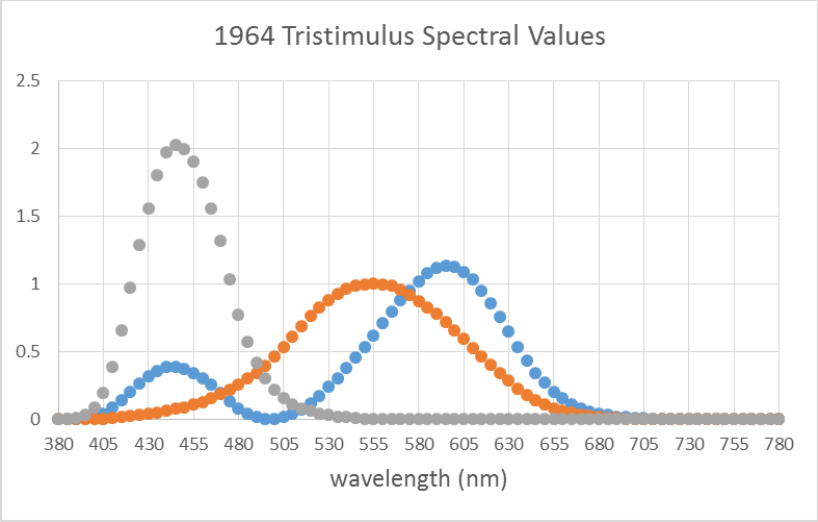

Figure 22. 1964 tristimulus spectral values (grey is Z, orange is Y, and blue is X)

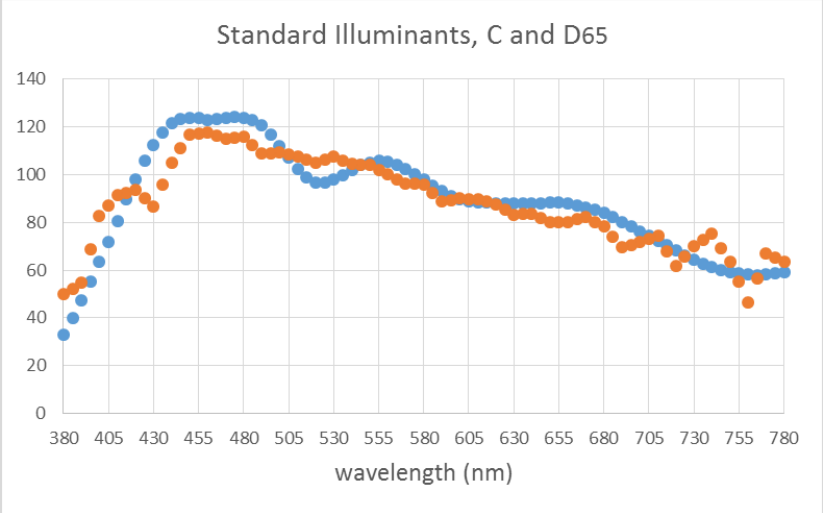

Figure 23. Spectra for standard illuminants C (blue) and D65 (orange)

8.3 Example

The transmission data on a CaF2 window (see Section 7, Transmittance) shows less transmission at short wavelengths than at long ones, indicating that there will be an increase in the yellowness of this broadband window. Putting the transmission data into the equations above and calculating the yellowness figures yields the values shown in Table 3.

Table 3. Yellowness values found from the measured transmittance of a CaF2 window

	CIE Standard Illuminant and Standard Observer				
	C, 1931	D_{65}, 1931	C, 1964	D_{65}, 1964	Average
YI	0.15	0.14	0.15	0.12	0.14

We ran a Monte Carlo analysis to determine the error in the yellowness calculation example for CaF2. We assumed a Gaussian distribution for each transmission measurement, with mean given by the theoretically predicted results and standard deviation based on the measured data variation. We approximated the standard deviation of the data from 380 to 400 nm to be 0.0029 and from 405 to 800 nm to be 0.0008. We then calculated one million transmission data sets and used the C, 1931 illuminant/observer combination to find one million yellowness results. The mean was 0.114 (slightly different from the result in Table 3 because this is idealized data) with a standard deviation of 0.028. So in this case the yellowness result, to two standard deviations, would be 0.114±0.056.

9 THE HARDWARE ASSEMBLY

As mentioned in Section 2, General Comments, the goal is to be able to perform all eight quantitative measurements (the six discussed in the preceding sections plus wavefront measurements, both normal and at 30 degrees to the windowpane) using the existing wavefront measurement system mounting hardware. The primary reason for this is that the windows are flight hardware and handling should be kept to a minimum. Once they are mounted into the wavefront measurement system X-Y scanner, which has gone through an engineering approval process allowing it to be used to mount flight window assemblies and panes, it would be prudent to attempt all of the measurements without having to remount the windowpane in a second holder. For more information on the X-Y scanner see NASA TM NESC-RP-14-00951, April 2016.

Figure 24 shows the complete measurement system. We have located the transmission measurement spectrometer under the platform on which the Zygo interferometer is located. The sources for the birefringence and haze measurements are located on either side of the interferometer while the haze and birefringence receivers are located on either side of the Zygo reference mirror. The transmittance system receiver is located below the reference mirror platform. The detection electronics are mounted on the surface of the optical table in the lower right.

Figure 24. System arrangement: Zygo interferometer and scanner, along with transmission measurement system, and haze and birefringence equipment

The hardware assembly was designed to provide as much clearance as possible from the flight windowpanes. The optical table is 10 feet long with the Zygo interferometer located on a 2 foot × 4 foot platform at one end. The scanner and reference mirror occupy the back 3 feet of the table, leaving about a 3-foot unoccupied region in front of the scanner. This area has been left free to provide the window handlers with sufficient clearance to place the windowpane (mounted in a holder) on the table before lifting it onto the scanner, without fear of touching the optical equipment. The measurement equipment was designed so that it would not intrude on this space.

Figure 25 shows the optical components behind the window/scanner, as seen through the scanner opening. The Zygo 6-inch-diameter reference mirror is a tenth-wavelength optical window that reflects only a small portion of the Zygo interferometer radiation back toward the measurement equipment; it looks like a window, but acts as a mirror. It is located on a 4-inch-thick optical platform lifted 15 inches above the optical table so that the entire area of a mounted window can be scanned. To the left of this mirror are the birefringence measurement receivers, and on both sides of the mirror are the haze receivers (mounted higher than the birefringence receivers). Below the optical platform is a 2-inch collecting lens used to focus the transmittance measurement beam onto a photodiode.

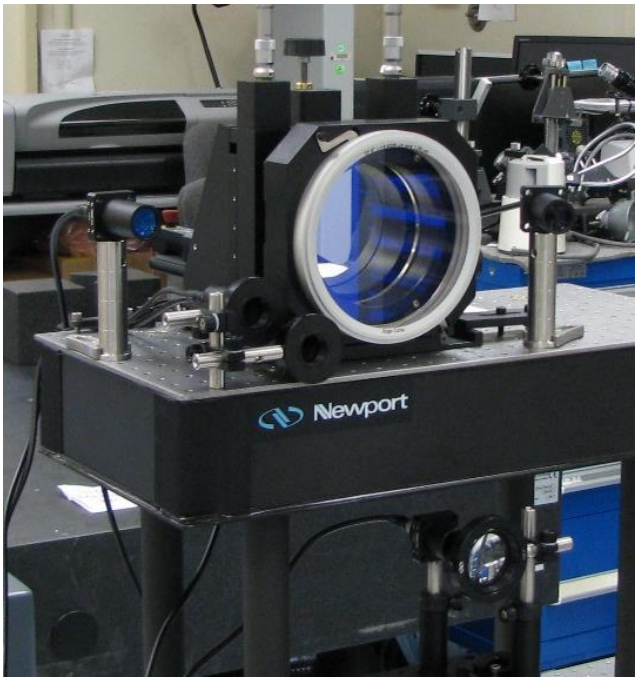

Figure 25. Optics on the far side of the windowpane, including the Zygo reference mirror, birefringence receivers (left), haze receivers (left and right), and transmittance lens and detector (bottom)

Figure 26 shows the optical components that generate light. The Zygo interferometer is on the top center of the optical platform, which is raised off the optical table by 15-inch legs. To the left of the Zygo interferometer are the laser and aperture used to provide a source for the haze measurement. To the right of the interferometer are the two sources of polarized light used to measure birefringence. Below the optical platform is the transmittance light source, consisting of a light source (small blue box) followed by a chopper and filter wheel attached to a monochromator. The light emerging from the interferometer is roughly collimated by a 2-inch-diameter lens with a 150 mm focal length, shown directly below the Zygo interferometer. The transmission measurement system is on its own platform, supported by 8-inch legs. Below this platform are the chopper wheel control module and power supplies. To the lower right are the current-to-voltage converter electronics connected by coaxial cables to the haze, birefringence, and transmittance photodetectors. The outputs from these modules are sent to the National Instruments analog-to-digital converter and then via a USB port to a computer.

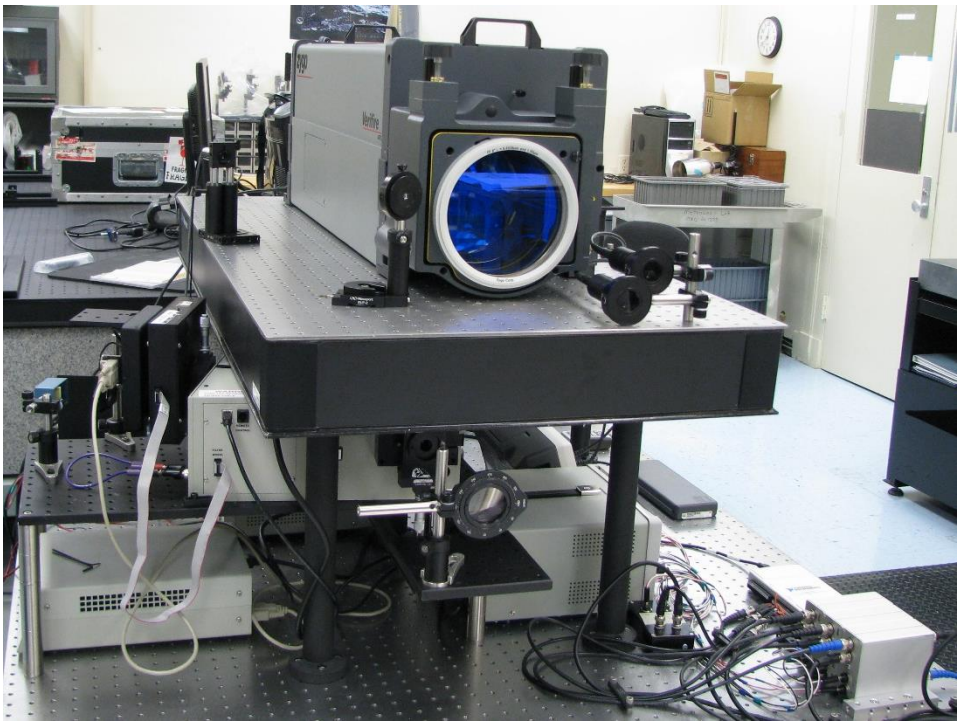

Figure 26. Zygo interferometer (top center), haze laser and aperture (top left), birefringence light sources (upper right), spectrometer equipment for measuring transmittance (left bottom and center bottom), and detection electronics (bottom right)

10 EXAMPLE OF SYSTEM OPERATION TEST

The test described in this section was run on a low-quality plastic window. The following are some observations about our measurement process:

a. The bulb used in the transmission measurement system must be warmed up for 2–3 hours before use.

b. The transmission system optical axis is much lower than the Zygo system axis. Consequently, most windowpanes can be lifted above the transmission system optical axis, allowing reference scans to be taken after the window has been mounted to the scanner. This means that the transmission measurements can be made anytime after the bulb has warmed up.

c. The haze measurement laser is required to have a 10-minute warm-up.

d. The haze standard measurement must be made before the window is mounted or after it is removed. To minimize drift errors, the haze measurement on the window is ideally taken within a short time of the haze standard measurement.

e. The birefringence system should be checked before the window is mounted, but we have not seen drift in this measurement. Consequently, it can be performed anytime in the process.

f. The Zygo wavefront measurements can be made anytime in the process.

Figure 27 shows a mock plastic windowpane mounted to the system X-Y scanner. We call this a *mock pane* because it was cut from an inexpensive piece of plastic and has poor optical properties, but it serves to highlight the performance of the measurement system.

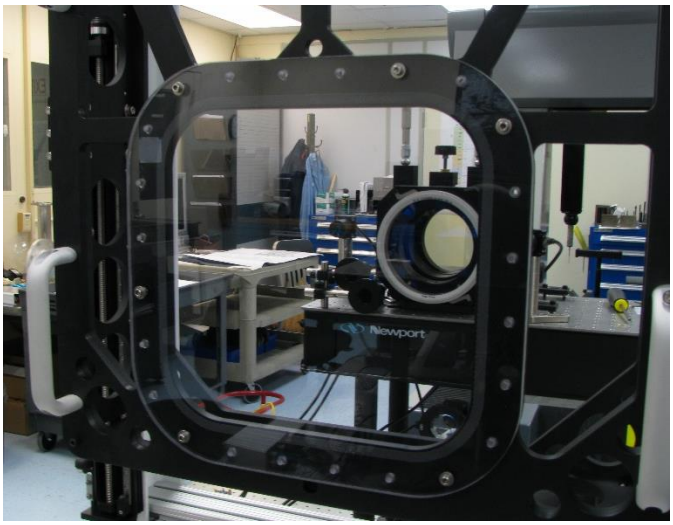

Figure 27. Mock plastic windowpane mounted to the X-Y scanner

The transmission through this plastic window is shown in Figure 28. Note that it does not transmit well below 400 nm and also has a notch in the deep red range (670–690 nm). Also, it has generally poor transmission through most of the visible range, with reasonable transmission in the near-infrared region. The luminous transmission is calculated to be 79%, which is low enough to cause this window to fail.

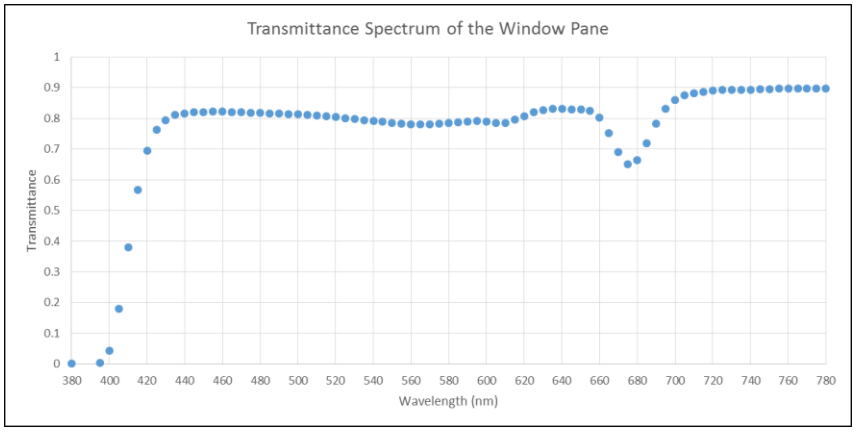

Figure 28. Transmission of the plastic pane

Using the transmission data, the reflection data can be derived as described above, but our process assumes minimal absorption from 450 to 800 nm, and this is not the case for this window. Consequently, we decided not to consider reflection data for this case.

Using the transmission data again, we can find the yellowness values for this plastic pane. These values, shown in Table 4, are all below the 0.5 yellowness pass/fail value, primarily because the absorption in the 670–690 nm range shifts the color balance away from the yellow, hence resulting in the negative numbers shown in the table.

Table 4. Yellowness values for the mock plastic windowpane

	CIE Standard Illuminant and Standard Observer				
	C, 1931	D_{65}, 1931	C, 1964	D_{65}, 1964	Average
YI	−0.97	−0.69	−0.27	0.14	−0.448

From above, haze is given by

$$h_P = 0.85\frac{(1.3*0.73*h_{P,1}+1.0*6.3*h_{P,2})}{(1.3*0.73*h_{s,1}+1.0*6.3*h_{s,2})}$$

Where the haze standard values are $h_{s,1}$ = 5.75 mV and $h_{s,2}$ = 0.39 mV. We measured from the plastic pane $h_{P,1}$ = 1.82 mV and $h_{P,2}$ = 0.3. Because the haze value for the plastic pane is 0.39±0.12, this pane likely passes the haze requirement.

Birefringence measurements were taken over a grid with 1 cm spacing, resulting in a 25 × 26 measurement array for each of the two polarization sensors. The results were processed as described above, yielding the retardance plot shown in Figure 29. Typical values are in the 180–200 nm/cm range, with significant outliers along the edges. This pane fails the birefringence requirement.

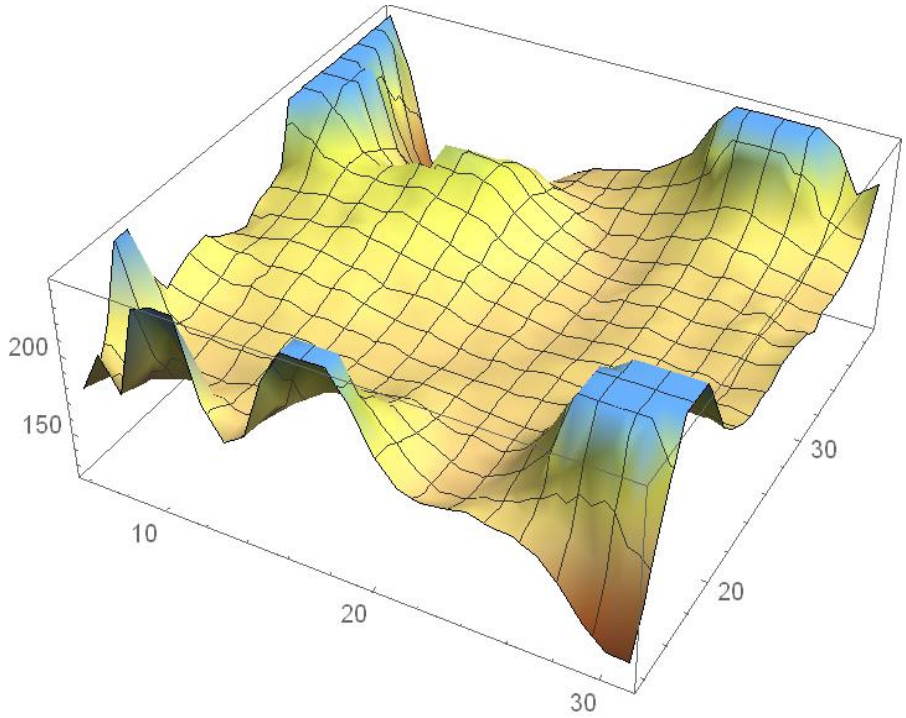

Figure 29. Birefringence of the plastic pane.

We took nine Zygo scans of this plastic pane, working in a 3 × 3 grid. The pane does not pass the wavefront criteria, which states that the peak-valley cannot be greater than 8 waves after removal of piston, tilt, and power. Figure 30 shows the best scan of the nine taken on this pane, where after removal of piston, tilt, and power, the peak-valley is 11.262. All of the other scans yielded higher peak-valley values; and in some locations, the pane affected the light so badly that the Zygo could not resolve the subsequent fringe pattern.

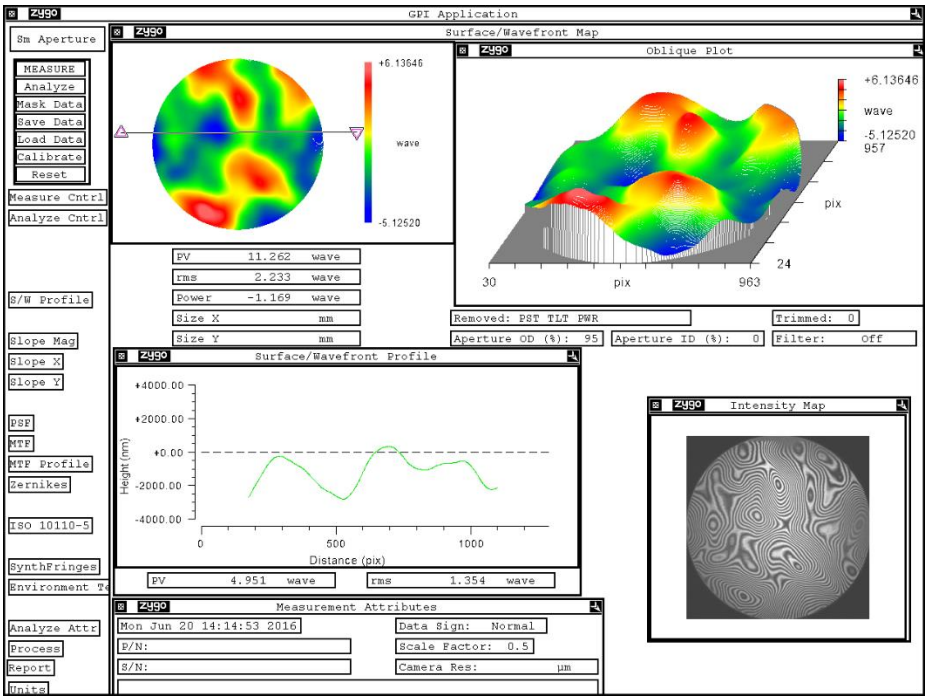

Figure 30. Best (lowest peak-valley) of the nine wavefront scans taken on the plastic pane

For each scan, a Zernike polynomial decomposition provides the tip/tilt information for this pane. Even though there is some overlap in the scans, we chose to weigh them each equally.

Table 5. Tip/tilt values from the nine Zygo scans.

Scan	Z_1	Z_2
1	−3.002	0.792
2	−7.120	2.252
3	−6.766	0.982
4	−6.032	1.155
5	−5.376	−1.12
6	−5.928	0.216
7	−3.323	0.029
8	−8.023	−0.720
9	−4.687	−2.013
Average	−5.584	0.175

Now, using the formula shown below, the wedge angle about the vertical axis is −0.108 arcmin (assuming an index of 1.5), and about a horizontal axis, it is 0.0034 arcmin.

$$\theta_{x,y}(\text{min}) = \frac{2Z_{1,2}\,0.633}{150*10^{3}}\,\frac{180}{3.14}\,\frac{60}{n} = 0.029\,\frac{Z_{1,2}}{n}$$

So the total wedge angle is only 0.108 arcmin, and it is located at an angle of about −1.8 degrees, measured from the horizontal axis. In other words, the plastic pane is thickest just below the horizontal axis to the left of the system, from the perspective of facing the Zygo interferometer. The plastic pane has very little wedge and passes that requirement.

REPORT DOCUMENTATION PAGE

Form Approved
OMB No. 0704-0188

1. REPORT DATE *(DD-MM-YYYY)*	2. REPORT TYPE	3. DATES COVERED *(From — To)*
18-08-2016	**Technical Memorandum**	**February 2016– July 2016**

4. TITLE AND SUBTITLE
Category B Plastic Pane Testing for JSC 66320 Rev A Requirements Verifiable through Acceptance Testing

5a. CONTRACT NUMBER

5b. GRANT NUMBER

5c. PROGRAM ELEMENT NUMBER

6. AUTHOR(S)
(1) Youngquist, Robert C.
(2) Nurge, Mark
(3) Danley, Susan
(4) Skow, Miles

5d. PROJECT NUMBER

5e. TASK NUMBER

5f. WORK UNIT NUMBER

7. PERFORMING ORGANIZATION NAME(S) AND ADDRESS(ES)
(1,2,3) National Aeronautics and Space Administration
Kennedy Space Center, FL 32899

(4) National Aeronautics and Space Administration
Johnson Space Center, TX 77058

8. PERFORMING ORGANIZATION REPORT NUMBER
NASA/TM–2016–xxxxxx

9. SPONSORING/MONITORING AGENCY NAME(S) AND ADDRESS(ES)
National Aeronautics and Space Administration
Washington, DC 20546-00001

10. SPONSORING/MONITOR'S ACRONYM(S)
NASA

11. SPONSORING/MONITORING REPORT NUMBER

12. DISTRIBUTION/AVAILABILITY STATEMENT
Unclassified – Unlimited **Distribution: Standard**
Subject Category:
Availability: NASA CASI (301) 621-0390

13. SUPPLEMENTARY NOTES

14. ABSTRACT

JSC 66320, Revision A, *Optical Property Requirements for Glasses, Ceramics, and Plastics in Spacecraft Window Systems*, lists several quantitative requirements that spacecraft windowpanes must meet. Recently, we were asked to establish a capability at the Kennedy Space Center to perform these measurements on category B plastic panes, i.e., plastic panes that could be used on a spacecraft for long-focal-length photography and piloting. Two of the criteria, normal wavefront and 30-degree wavefront attributes, can be measured with existing equipment and processes (see NASA TM NESC-RP-14-00951, April 2016) and are not discussed in this document. However, the other six criteria—haze, wedge angle, birefringence, reflectance, transmittance, and color balance—required substantial development and are the subject of this document.

15. SUBJECT TERMS
spacecraft windowpanes, spacecraft window systems, optical metrology, birefringence

16. SECURITY CLASSIFICATION OF:			17. LIMITATION OF ABSTRACT	18. NUMBER OF PAGES	19a. NAME OF RESPONSIBLE PERSON
a. REPORT	b. ABSTRACT	c. THIS PAGE			**Robert C. Youngquist**
U	**U**	**U**	**UU**	**52**	19b. TELEPHONE NUMBER *(Include area code)* **(321) 867-1829**